

POLYACRYLATES WITH 4'-(N,N-DIMETHYLAMINO)-
STILBENE-4-CARBOXYLIC ESTER
SIDE CHAINS

By

MINGYANG ZHAO
||

Bachelor of Science
Qinghua University
Beijing, P. R. China
1978

Master of Engineering
Beijing Research Institute
of Chemical Industry
Beijing, P. R. China
1984

Submitted to the Faculty of the
Graduate College of the
Oklahoma State University
in partial fulfillment of
the requirements for
the degree of
MASTER OF SCIENCE
December, 1989

Thesis
1989

2627P

cop. 2

POLYACRYLATES WITH 4'-(N, N-DIMETHYLAMINO)-
STILBENE-4-CARBOXYLIC ESTER
SIDE CHAINS

Thesis Approved:

Warren T. Ford

Thesis Adviser

Christopher M. Davis

H. Olin Spirey

Noeman N. Durham

Dean of the Graduate College

ACKNOWLEDGMENTS

It is a pleasure and good fortune to study in the Department of Chemistry, at Oklahoma State University. I wish to express my sincere gratitude to the faculty and staff members who assisted me in this project and during my coursework at Oklahoma State University. In particular, I wish to thank Dr. Warren T. Ford, my advisor, for his intelligent guidance and support, his instruction and patience are forever appreciated. I am also grateful to Dr. Christopher M. Adams and Dr. H. Olin Spivey for serving on my graduate committee.

I express my thanks to Dr. David Tatarsky for assistance with preliminary polarizing microscopy and DSC experiments and Dr. Roger Reeves for the SHG experiment in the laboratory of Dr. Richard C. Powell, OSU Department of Physics. I also extend my thanks to all members of our research group for their help and friendship.

Special thanks go to my wife, Hui Yu, for her love and encouragement, to my father and mother for all they had to sacrifice during my graduate work.

TABLE OF CONTENTS

Chapter	Page
I. INTRODUCTION	1
II. EXPERIMENTS	11
Materials	11
Techniques	11
Methyl 4-(chloromethyl)benzoate	12
Diethyl <i>p</i> -Carbomethoxybenzylphosphonate	13
4-Carbomethoxy-4'-dimethylamino- <i>trans</i> -stilbene (<i>trans</i> -CMS)	13
4-Carbomethoxy-4'-dimethylamino- <i>cis</i> -stilbene (<i>cis</i> -CMS)	14
ω -Hydroxyalkyl 4'-Dimethylamino- <i>trans</i> -stilbene-4-	
carboxylate (A-n)	14
Acrylate Monomers (M-n)	15
Acrylate Polymers (P-n)	15
Polymer Film Making	16
III. RESULTS	26
Synthesis	26
Liquid Crystal Properties of Alcohols (A-n)	
and Monomers (M-n)	28
Liquid Crystal Properties of Polymers (P-n)	29
Polymer film making	51
IV. DISCUSSION	52
REFERENCES	61

LIST OF TABLES

Table	Page
I. Side chain liquid crystalline polymers for NLO	6
II. ^1H NMR chemical shifts in spectra of CMS , A-n , M-n , and P-10 . . .	18
III. ^{13}C NMR chemical shifts in spectra of CMS , A-n , M-n , and P-10 . . .	20
IV. UV-vis spectral data	23
V. Characterization of CMS , A-n , and M-n	24
VI. Characterization of polymers.	25
VII. Relation of thickness and rotating speed from spin-coating of 10% P-10B in 1, 4-dioxane	51
VIII. Comparison of polyacrylates.	57
IX. Comparison of acrylate monomers	58

LIST OF FIGURES

Figure	Page
1. Thermal behaviour of low molar mass liquid crystals and side chain polymer liquid crystals	2
2. Schematic of side chain liquid crystal polymer for second order nonlinear optics.	4
3. Target polymers.	9
4. UV-vis absorption spectra of CMS	22
5. DSC thermograms of A-2, M-2 and P-2	30
6. DSC thermograms of A-4, M-4 and P-4	31
7. DSC thermograms of A-6, M-6 and P-6	32
8. DSC thermograms of A-8, M-8 and P-8	33
9. DSC thermograms of A-10, M-10 and P-10	34
10. Polarizing microphotograph of A-4	35
11. Polarizing microphotograph of A-6	36
12. Polarizing microphotograph of A-8	37
13. Polarizing microphotograph of A-10	38
14. Polarizing microphotograph of M-4	39
15. Polarizing microphotograph of M-6	40
16. Polarizing microphotograph of M-8	41

Figure	Page
17. Polarizing microphotograph of M-10	42
18. Polarizing microphotograph of P-4	43
19. Polarizing microphotograph of P-6	44
20. Polarizing microphotograph of P-8	45
21. Polarizing microphotograph of P-10	46
22. Dependence of melting and isotropic transition temperatures of monomers M-n on spacer length.	47
23. Dependence of glass and isotropic transition temperatures of polymers on carbon spacer length	48
24. DSC thermogram of P-8B with different thermal histories	50
25. Dependence of molar isotropization enthalpies of polymers on the number of spacer carbons	53
26. Dependence of phase transition on mass fraction of polar core.	54

ABBREVIATIONS

A-n	intermediate alcohols with n alkyl carbons
CMS	4-carbomethoxy-4'-(N,N-dimethylamino)stilbene
G	glass
I	isotropic
K	crystal
LC	liquid crystal
LCP	liquid crystalline polymer
M-n	acrylate monomers with n alkyl carbons
N	nematic
NLO	nonlinear optical
P-n	acrylate polymers with n alkyl carbons
S	smectic
S _A	smectic A
S _C	smectic C
SHG	second harmonic generation
T _g	glass transition temperature
T _i	isotropic transition temperature
T _m	melting temperature

CHAPTER I

INTRODUCTION

About ten years ago, a clever new idea made it possible to combine two individual classic scientific fields, polymers and liquid crystals, to form an attractive new field.^{1,2} The new idea was to attach a low molar mass liquid crystal to a polymer backbone via a flexible spacer to get a new material, a side chain liquid crystalline polymer (LCP). Since then this new scientific field has experienced rapid growth. Each year hundreds of new polymers having liquid crystalline properties are synthesized and investigated. Liquid crystalline polymers combine the properties of both polymers and liquid crystals. As polymers they have the advantages of processability into almost any shape and the mechanical properties of plastics. As liquid crystals these polymers are neither solid nor liquid. They can flow as liquids, but they are not isotropic. They have periodic ordered arrangements of structural units, but their order is only one or two dimensional, not three dimensional as in a crystalline solid. The partial order makes these polymer liquid crystals anisotropic to light and to electric and magnetic fields. The thermal behavior of liquid crystalline polymers is different from that of low molar mass liquid crystals.^{3,4} For low molar mass compounds the liquid crystalline state, also called mesophase, is observed from the melting temperature (T_m) to the isotropic temperature (T_i). For a noncrystallizable side chain LCP the low temperature limit of the LC state is the glass transition temperature (T_g), above which the so-called segmental mobility is exhibited. In an interval between T_g and T_i the polymer is either in the form of an elastomer or in the form of a viscous melt in a LC

state. In contrast to a low molar mass liquid crystal, which usually crystallizes on cooling, a side chain LCP undergoes a glass transition on cooling. So the glassy state retains the order of the mesophase (Figure 1).

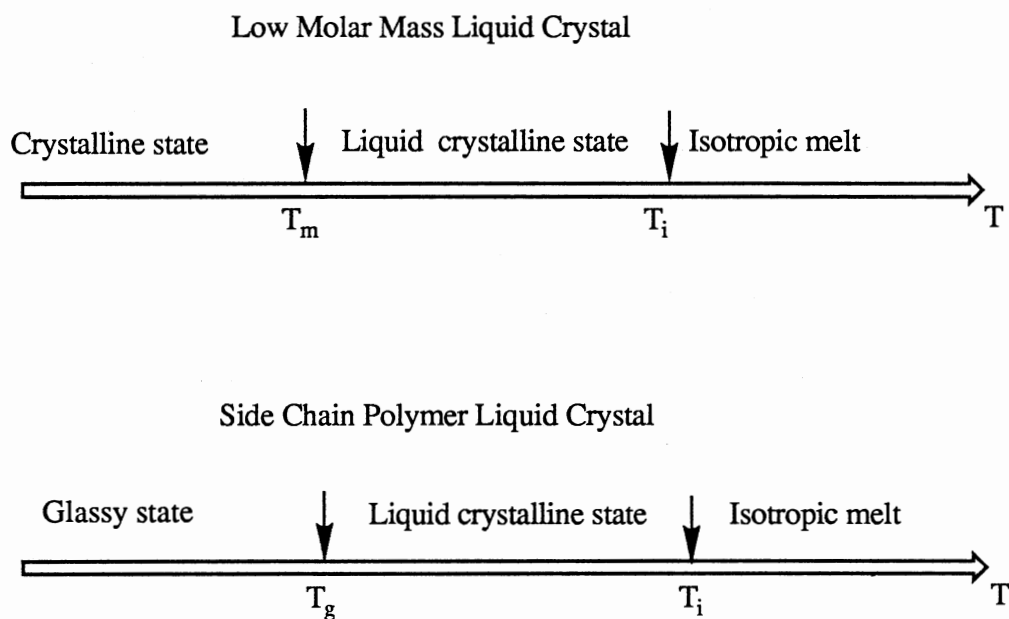


Figure 1. The thermal behavior of low molar mass liquid crystals and side chain polymer liquid crystals.

The special properties of LCP's made them promising materials in many applications, particularly in the area of electrooptical displays and nonlinear optical (NLO) materials.⁵⁻¹⁸ Nonlinear optical materials are substances exhibiting nonlinear polarizations in an electric, magnetic or electromagnetic field. When an electromagnetic field acts on these materials the oscillating field polarizes the materials. The positive and negative

charges in the constituent molecules move in opposite directions, so that an oscillating electric dipole is induced in the materials. The induced dipole per unit volume is called the polarization, P . If the polarization is linearly proportional to the strength of the electromagnetic field the optical response is called linear. For nonlinear optical materials the induced polarization also depends on higher powers of the field strength. Generally the induced polarization component P_i can be written as

$$P_i = P_{o,i} + \chi_{ij}^{(1)}E_j + \chi_{ijk}^{(2)}E_jE_k + \chi_{ijkl}^{(3)}E_jE_kE_l + \dots$$

where P_i is the i th component of the polarization, $P_{o,i}$ is the permanent polarization, $\chi^{(1)}$ is the linear electronic susceptibility, $\chi^{(2)}$ is the second order nonlinear electronic susceptibility, and $\chi^{(3)}$ is the third order nonlinear electronic susceptibility. In recent years it has been found that organic polymers may exhibit better NLO properties than the conventional inorganic single crystals. In this work the research focus is on the side chain polymers with large second order susceptibility. Such polymers might be used in optical communication and computing systems for fast switches to modulate wave carrying information and to amplify signals.

For a LCP to display second order NLO properties, the bulk phase of the LCP substrate must have a macroscopic noncentrosymmetric structure. Electric field poling or the Langmuir-Blodgett deposition technique can be used to obtain a bulk polymer material arranged in a noncentrosymmetric manner macroscopically. One second order NLO property is second harmonic generation (SHG), the doubling of the frequency of a laser beam. Experimentally a pulsed laser beam is directed through the LCP film, and the power conversion of the incident radiation into the second harmonic is determined.

The structure of a side chain liquid crystalline polymer designed for second order NLO properties is a combination of a mesogen (LC unit, the structural unit that may lead to

a liquid crystalline phase), a NLO chromophore (NLO unit), a spacer and a polymer backbone. A typical NLO side chain liquid crystalline polymer is illustrated in Figure 2.

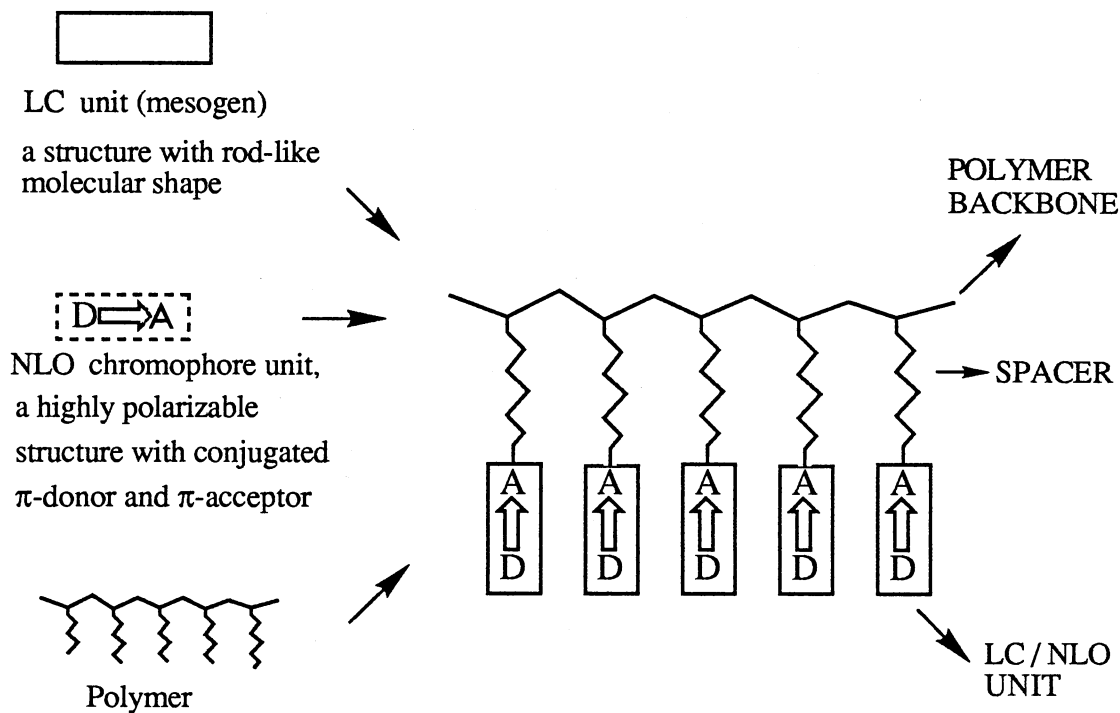


Figure 2. Schematic of side chain liquid crystalline polymer for second order nonlinear optics.

In these polymers the pendant LC/NLO unit is connected to the polymer backbone, e. g. an acrylic or methacrylic ester, or a siloxane, by a flexible spacer group, often a polymethylene chain. The polymer backbone distinguishes a polymer liquid crystal from a

low molar mass liquid crystal. Attachment of low molar mass liquid crystal to the macromolecular chain usually increases the temperature range of the LC state. The high viscosity of a polymer mesophase results in slowing down of all structural rearrangement and hardening of the ordered structure below T_g . The mesogenic unit is characterized by a large axial ratio, which is often realized by rod-like chemical structures having para-substituted aromatic rings, and rigid central linkages between the rings. The NLO chromophore designed for second-harmonic-generation is a highly polarizable π -electron conjugated structure with an electron-rich donor group on one end and an electron-deficient acceptor group on the other end. The spacer is a flexible aliphatic chain. Its function is to decouple the side chain motion from that of the polymer backbone. Otherwise the latter will affect the stability of the liquid crystal phase. The spacer also has a plasticizing effect on a LCP. An increase in the spacer length shifts the T_g toward lower temperature. By appropriate design of these structural units, it is possible to produce a variety of polymers with different nonlinear optical activities, and liquid crystal properties. The mesophases of LCP's may be nematic (N) with one-dimensional order or smectic (S) with two-dimensional order. There are nine different smectic phases (S_A , S_B , S_C , ... S_I), of which the most common are S_A and S_C . In these two mesophases the molecules are parallel to one another and are arranged in layers. In a S_A phase the molecular long axes are perpendicular to the layer plane; in a S_C phase the long axes are tilted. The liquid crystallinity, also called mesomorphism, can be examined by differential scanning calorimetry, polarizing microscopy, X-ray diffraction and other techniques. Usually the higher viscosity and broader temperature ranges of the LCP phase transitions make the investigation of mesomorphism more difficult than with low molar mass liquid crystals.

Table 1 presents the NLO side chain liquid crystalline polymers which have been reported in the literature to July 1989.

TABLE I
SIDE CHAIN LIQUID CRYSTALLINE POLYMERS FOR NLO

Polymer	Phase transition		Ref.
	T _g (°C)	T _i (°C)	
$\begin{array}{c} \text{CH}_2 \\ \\ \text{CH}_3-\text{C}-\text{CO}_2(\text{CH}_2)_n\text{O}-\text{C}_6\text{H}_4-\text{C}_6\text{H}_4-\text{NO}_2 \\ \\ \text{---} \end{array}$			7
n=3	85	110	N
n=5	45	72	N
n=6	40	64	N
n=8	35	75	N
n=11	20	95	S _A
n=12	10	80	S _A
$\begin{array}{c} \text{CH}_2 \\ \\ \text{CH}_3-\text{C}-\text{CO}_2(\text{CH}_2)_6\text{O}-\text{C}_6\text{H}_4-\text{N}=\text{C}=\text{C}_6\text{H}_4-\text{NO}_2 \\ \\ \text{---} \end{array}$			15
$\begin{array}{c} \text{CH}_2 \\ \\ \text{CH}_3-\text{C}-\text{CO}_2(\text{CH}_2)_6\text{O}-\text{C}_6\text{H}_4-\text{CO}-\text{C}_6\text{H}_4-\text{C}(\text{CN})=\text{C}_6\text{H}_4-\text{CH}_3 \\ \\ \text{---} \end{array}$	118	206	N
$\begin{array}{c} \text{CH}_2 \\ \\ \text{H}-\text{C}-\text{CO}_2(\text{CH}_2)_6\text{O}-\text{C}_6\text{H}_4-\text{CO}-\text{C}_6\text{H}_4-\text{CN} \\ \\ \text{---} \end{array}$			
$\begin{array}{c} \text{CH}_2 \\ \\ \text{H}-\text{C}-\text{CO}_2(\text{CH}_2)_6\text{O}-\text{C}_6\text{H}_4-\text{N}=\text{C}=\text{C}_6\text{H}_4-\text{CN} \\ \\ \text{---} \end{array}$	25	110	N

TABLE I (continued)

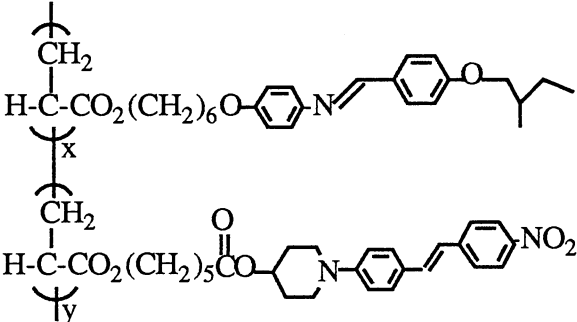
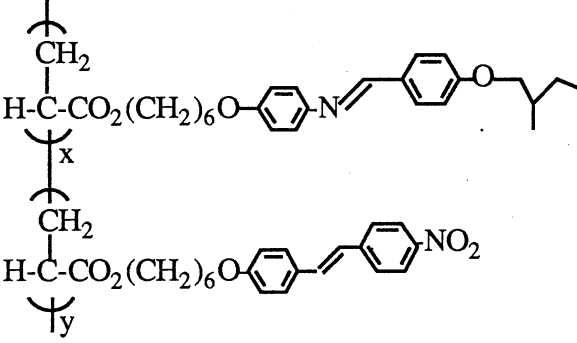
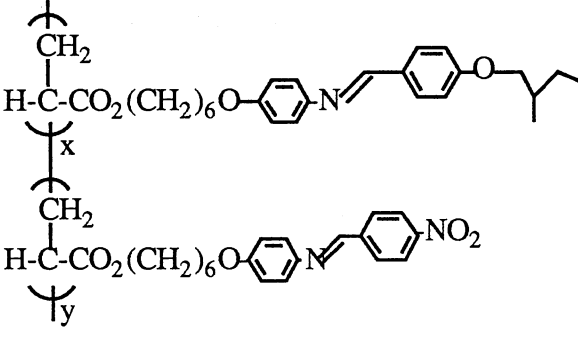
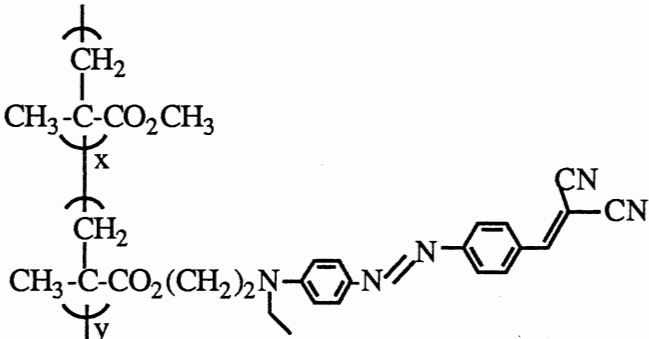
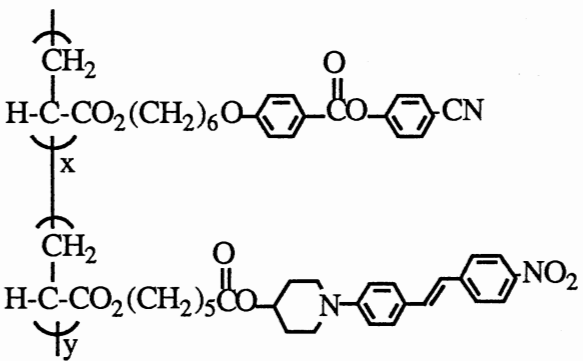
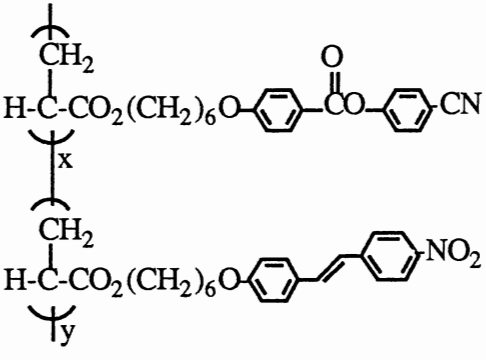
Polymer	Phase transition T _g (°C) T _i (°C)		Ref.	
			Phase	
	75	147	N	6
	71	184	N	6
	43	160		6

TABLE I (continued)

Polymer	Phase transition		Ref.
	T_g ($^{\circ}\text{C}$)	T_1 ($^{\circ}\text{C}$)	
	127		18
	55	110	N 13
	44	91	N 13

To study the relationship between structure, mesomorphic properties and NLO activities, a series of new polyacrylates with polarized stilbene side chains was designed. The target polymer is given in Figure 3.

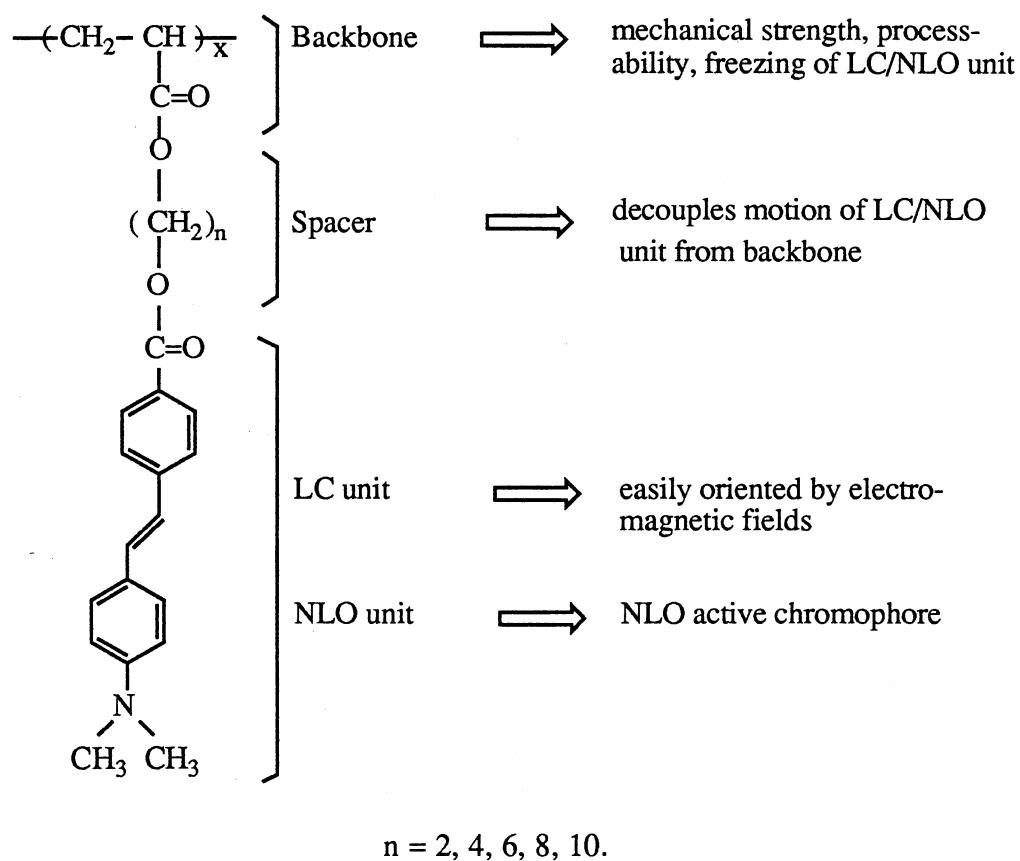


Figure 3. Target polymers

The reason to choose a polarized stilbene as both the mesogen and NLO chromophore is that the stilbenes have some versatile properties. The rod-like molecular structure makes stilbenes an important class of liquid crystalline compounds.^{19, 20} Push-pull stilbene derivatives with a donor group at one end and an acceptor group at the other end have been reported to have large second order nonlinear susceptibilities.^{21, 22} By appropriate design it is possible to obtain the stilbene derivatives with both liquid crystalline properties and NLO properties.²³ The new polymers contain a strong π -electron donating dimethylamino group at one end of the stilbene, and an electron-accepting ester group at the other end. This structure is expected to exhibit both NLO and LC properties. The highly polar 4'-(N,N-dimethylamino)stilbene-4-carboxylic ester group will influence the liquid crystal properties, since the mesogenic properties of a compound are a consequence of the balance between intermolecular attractive and repulsive forces, which depend upon anisotropy of polarizability, dipole moment and steric effects. The influence of polar mesogenic groups on low molar mass liquid crystal properties has been studied.^{24, 25} It was found that there is a correlation between nematic-isotropic transition temperatures and polarizability, steric effects and dipole moments of the polar substituents. A highly polar substituent raises the nematic-isotropic transition temperature.

In this thesis the synthesis and characterization of the new monomers and polymers is reported. The study of novel polar polymer materials will help in the understanding of the relationships between structure and mesomorphic properties, and structure and NLO activities. A better understanding will help the design and development of new polymers with desired liquid crystal properties and enhanced nonlinear optical activities.

CHAPTER II

EXPERIMENTAL

Materials. 4-(N,N-Dimethylamino)benzaldehyde was recrystallized from ether. Acryloyl chloride and triethylamine were distilled under argon. 2,2'-Azobisisobutyronitrile (AIBN) was recrystallized from methanol. Tetrahydrofuran (THF) and 1,4-dioxane were refluxed over sodium and distilled under nitrogen. All of the other reagents and solvents were used as received.

Techniques. NMR spectra were recorded on a Varian XL-300 instrument at 300 MHz for ^1H or 75.43 MHz for ^{13}C . All spectra were recorded in CDCl_3 solution with TMS as internal standard unless otherwise specified. IR spectra were taken on a Perkin Elmer 681 infrared spectrophotometer with KBr disks. UV-visible spectra were taken on a Varian DMS 200 UV-visible spectrophotometer. Elemental analyses were done at Desert Analytics Organic Microanalysis (Tucson, Arizona). TLC was performed with silica gel GF thin layer chromatography plates (Analtech Inc.) with mixtures of petroleum ether and ethyl acetate as solvents. High pressure liquid chromatographic (HPLC) analyses were performed with a Waters 590 pump equipped with a normal phase 5 μm silica column (length x ID = 250 mm x 4.6 mm, Whatman PARTISIL 5), a Rheodyne injector with a 20 μL sample loop, a Beckman 153 analytical 254 nm UV detector, and an Interactive Microware data station. The eluant was 9/1 (v/v) hexane/ethanol. Molecular weights were determined by gel permeation chromatography (GPC) with the same Waters 590 pump

using two PL gel columns of 10^3 \AA and 10^4 \AA (particle size: 10 \mu m , length x ID = $300 \text{ mm} \times 7.5 \text{ mm}$, Polymer Lab. Ltd.). THF was used as solvent (1 mL/min , $25 \text{ }^\circ\text{C}$), and polystyrenes of $M_n = 0.8 - 233 \times 10^3$ were used as the standards for calibration. Thermal transitions were determined with a Perkin-Elmer DSC-2C differential scanning calorimeter equipped with a TADS 3600 data station. Heating and cooling rates were $20 \text{ }^\circ\text{C/min}$, unless noted otherwise. The thermal transitions were read at the maximum of the endothermic or exothermic peaks. After the first heating and cooling scans, the polymer sample was annealed at about $10 \text{ }^\circ\text{C}$ below the isotropization temperature for about 30 min, cooled to $25 \text{ }^\circ\text{C}$ at $20 \text{ }^\circ\text{C/min}$, and scanned for the data that are reported. Glass transition temperatures (T_g) were read at the midpoint of the change in the heat capacity. The temperature and ΔH were calibrated with indium as the standard. The thermal transitions and anisotropic textures were observed on a Nikon 104 optical polarizing microscope fitted with a Nikon N-2000 35 mm automatic camera and an Instec hot stage that was controlled by an Apple IIe computer.

Methyl 4-(chloromethyl)benzoate (MCB). Method A. Thionyl chloride (83.3 g, 700 mmol) was added dropwise to methyl 4-(hydroxymethyl)benzoate (83.1 g, 500 mmol) cooled in an ice-water bath. The reaction mixture was heated slowly and refluxed for 10 h. The solution was poured into 500 mL of cold water and stirred, and the mixture was extracted with two 150 mL portions of ether. The combined ether extracts were washed twice with 150 mL of saturated aqueous sodium bicarbonate and once with 150 mL of water. The washed extracts were dried over 25 g of anhydrous sodium sulfate and concentrated with a rotary evaporator. The residue was distilled (bp $109 \text{ }^\circ\text{C}$ at 10 mmHg). After recrystallization from hexane, 74.1 g (80.3%) of colorless needle crystals was obtained: mp $38\text{-}39 \text{ }^\circ\text{C}$ (lit.²⁶, mp $39\text{-}40 \text{ }^\circ\text{C}$).

Method B. 4-Chloromethylbenzoic acid (80.0 g, 580 mmol) and concentrated sulfuric acid (64 mL) were dissolved in 900 mL of methanol. The solution was refluxed

for 1.5 h under an argon atmosphere. Afterwards the reaction mixture was poured into 1 L of water and stirred. The mixture was extracted twice with 350 mL of benzene. The organic layer was washed with water and with two 350 mL portions of saturated sodium bicarbonate, and dried over sodium sulfate. The organic solution was evaporated with a rotary evaporator. The remaining oil was distilled (bp 109 °C at 10 mmHg) to give 83.0 g (95.9%) of colorless needle crystals: mp 38-39 °C.

Diethyl *p*-Carbomethoxybenzylphosphonate. Methyl 4-(chloromethyl)benzoate (36.9 g, 200 mmol) and triethyl phosphite (36.6 g, 220 mmol) were stirred and refluxed for 1 h under argon. Elimination of ethyl chloride started at about 130 °C. As the reaction proceeded the temperature of the solution rose to 187 °C. At reduced pressure, the excess triethyl phosphite was distilled out, and 52.5 g (92.0%) of colorless viscous liquid product was obtained at 185 °C/5 mmHg. ¹H NMR: d 1.26 (t; 6H, -O-CH₂-CH₃), 3.24 (d; 2H, -PO-CH₂-Ph-), 3.90 (s; 3H, CH₃-O-), 4.04 (m; 4H, -O-CH₂-CH₃), 7.4, 8.0 (m; 4H, aromatic protons). ¹³C NMR: d 16.4 (-OCH₂CH₃), 33.9 (Ph-CH₂-PO-), 52.0 (CH₃-O₂C-), 62.2 (-OCH₂CH₃), 128.8, 129.8, 137.3 (aromatic), 166.8 (CH₃-O₂C-).

4-Carbomethoxy-4'-dimethylamino-*trans*-stilbene (*trans*-CMS). The reaction was done in the dark in an argon atmosphere. A solution of 4-(*N,N*-dimethylamino)benzaldehyde (3.0 g, 20 mmol) and diethyl *p*-methoxy-carbonybenzylphosphonate (5.7 g, 20 mmol) in 30 mL of THF was added dropwise to a stirred slurry of sodium hydride (0.70 g, 30 mmol) in 60 mL of THF containing 15-crown-5 ether (30 mg) at 0 °C. Hydrogen evolved rapidly, and a yellow precipitate formed. The suspension was stirred for 2 h at 25 °C and poured into 400 mL of ice water. The precipitate was filtered and washed with ether. After recrystallization from *N,N*-dimethylformamide (DMF), 4.4 g (78%) of luminescent yellow crystals was obtained: mp 220-222 °C (lit.²⁷, mp 217-218 °C). NMR data are in Table II and Table III. IR: 1710

cm^{-1} (C=O), 960 cm^{-1} (C-H). UV-visible spectra of CMS are given in Figure 4 and Table IV.

4-Carbomethoxy-4'-dimethylamino-*cis*-stilbene. (*cis*-CMS) The *cis*-isomer was prepared by photoisomerization of the *trans*-CMS. *trans*-CMS (0.30 g) was dissolved in 50 mL of chloroform and exposed to normal room fluorescent lights for two days. Two spots were detected by TLC using 7% ethyl acetate and 93% petroleum ether as the solvent. For the *cis*-isomer $R_f = 0.27$; for the *trans*-isomer $R_f = 0.20$. The ^1H NMR spectrum showed that the solution was composed of 74% *cis*-isomer and 26% *trans*-isomer. The mixture solution was placed on a silica gel chromatographic column (2.5 x 50 cm, 60-200 mesh), and the *cis*-isomer was eluted with 7/93 (v/v) ethyl acetate/petroleum ether. After evaporation and crystallization from benzene 0.10 g of crystals was obtained, which contained 94% *cis*-isomer and 6% *trans*-isomer as determined from the ^1H NMR spectrum. The NMR data are in Table II and Table III. IR: 1720 cm^{-1} (C=O), 715 cm^{-1} (C-H). The UV-visible spectra are given in Figure 4 and Table IV.

ω -Hydroxyalkyl 4'-dimethylamino-*trans*-stilbene-4-carboxylates (A-n) All five intermediate alcohols (A-n) were synthesized by the transesterification of 4-carbomethoxy-4'-dimethylamino-*trans*-stilbene with excess diol in the presence of concentrated sulfuric acid. A typical procedure is illustrated with the synthesis of A-8. *trans*-CMS (11.2 g, 40 mmol), 1,8-octanediol (200 g, 1.37 mol), and concentrated sulfuric acid (3.5 mL) were stirred at $90 \text{ }^\circ\text{C}$ for 36 h under argon in the dark. The reaction was monitored by TLC using 1:1 ethyl acetate and petroleum ether as the solvent. The solution was poured into 2 L of water and stirred. The yellow precipitate was filtered and recrystallized from methanol to yield 9.8 g (62%) of yellow product with a purity of 99% (HPLC). IR: $3440\text{-}3520 \text{ cm}^{-1}$ (O-H). The ^1H NMR and ^{13}C NMR chemical shifts for all compounds together with their yields and thermal analyses are presented in Table II, Table III and Table V.

Acrylate Monomers (M-n). All five acrylate monomers were synthesized by the esterification of the corresponding alcohols (A-n) with acryloyl chloride. For example, **M-8** was prepared by the following procedure. Under argon in the dark **A-8** (9.20 g, 23 mmol), triethylamine (5.10 g, 50 mmol) and 300 mL of THF were stirred at 0 °C. Acryloyl chloride (4.80 g, 50 mmol) was added dropwise. The mixture was allowed to warm to 25 °C and stirred for 12 h. The reaction was monitored by TLC with 1:1 ethyl acetate and petroleum ether as the solvent. The yellow suspension was poured into 2 L of water and stirred. The precipitated product was filtered and recrystallized from methanol to give 9.0 g (86%) of yellow crystals with a purity higher than 99.0% (HPLC). There was no O-H stretching band in the infrared spectrum. The ^1H NMR and ^{13}C NMR chemical shifts for all monomers and other characterizations are presented in Table II, Table III and Table V.

Acrylate Polymers (P-n). Method A (for **P-2**, **P-4**, **P-6**, **P-8** and **P-10**). The acrylate monomers (**M-n**), each 0.50 g, were polymerized in sealed glass tubes with 1 wt % AIBN as initiator and 1,4-dioxane as solvent. The monomer concentration was 10% (wt/v). The monomer solution was degassed by three freeze-pump-thaw cycles under vacuum before the tube was sealed by gas-oxygen torch under an argon atmosphere. The sealed tube was held in a water bath at 60 °C for 60 h. The reaction solution was poured into methanol to precipitate the polymer. The polymer was filtered, dried under vacuum, and purified by reprecipitation from THF solution into methanol. The yields and characterization of the polymers are reported in Table VI.

Method B (for **P-8B** and **P-10B**). The monomers **M-8** (8.40 g) and **M-10** (12.50 g) were separately dissolved with 1 wt % of AIBN into 76 mL and 104 mL of 1,4-dioxane contained in two 200 mL flasks equipped with reflux condensers. The solutions were purged with argon for 2 h and heated at 65 °C for 96 h. After polymerization the solutions were poured into methanol to precipitate the polymers. The polymers were filtered

and dried under vacuum to yield 5.47 g (65%) and 7.8 g (62%).of crude products. After reprecipitation from THF solution into methanol 2.63 g (31%) of polymer **P-8B** and 5.11 g (41%) of polymer **P-10B** were obtained. GPC analyses was used to monitor the removal of monomer from polymer during the precipitation procedure. After the last precipitation GPC analyses showed no peaks for residual monomers in any of the polyacrylates reported in Table VI.

Polymer Film Making. Polymer solutions in 1,4-dioxane (10% wt/v) were sonicated and filtered through a 5 μm filter (Millex-SR). Indium-tin-oxide (ITO) coated conductive glass (Applied Films Lab. Inc.) was cleaned by washing with sulfuric acid (96%), *n*-amyl alcohol, and isopropyl alcohol with a deionized water rinse after each washing step, and dried in a vacuum desiccator. The polymer films were spin coated with a 1-PM101D-R485 photoresist spinner (Headway Research Inc.) onto 25 x 20 mm pieces of ITO glass. The films were dried under vacuum.

The thickness of the film was calculated from the weight and density of the polymer ($d = 1.169 \text{ g/cm}^3$ for **P-8B**, $d = 1.155 \text{ g/cm}^3$ for **P-10B**). The density of the polymer was measured at 25 $^{\circ}\text{C}$ by determining the weight of a calibrated pycnometer filled with heptane ($d = 0.684 \text{ g/cm}^3$) in which a certain quantity of the polymer sample was immersed.²⁸ The sample volume equals the pycnometer volume minus the undisplaced volume of heptane.

Noncentrosymmetric orientation in the polymer films was obtained by poling the films in a DC electric field. The 0.5 - 3.0 mm thick films were covered with a second ITO electrode. A wire was attached to each of the conductive glass surfaces using electrically conductive epoxy adhesive (SL100-ZX, Zymet). The assembly was placed on the microscope hot stage. The film first was heated above the isotropization temperature for 10 min, and then the assembly was cooled at a rate of 0.2 $^{\circ}\text{C}/\text{min}$ to a temperature about 5 $^{\circ}\text{C}$ below the T_i and maintained at this temperature for 24 h. A DC electric field was applied at

40-80 V/ μm . After 24 h the film was rapidly cooled to 25 °C in the presence of the electric field. Second harmonic generation experiments with the poled films were performed by Dr. Roger Reeves of the OSU Department of Physics. He observed a second harmonic signal at 532 nm with a 1064 nm Nd:YAG laser. The experiments and results will be reported later.

TABLE II

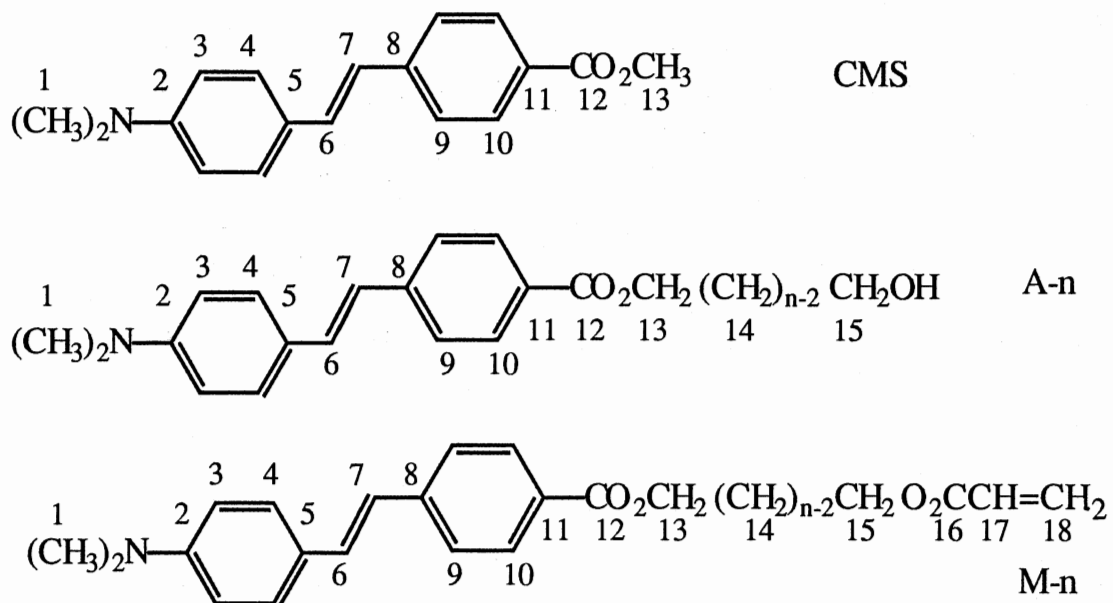
¹H NMR CHEMICAL SHIFTS IN SPECTRA OF CMS, A-n, M-n, AND P-n.

TABLE II (continued)

	1	3	4	6	7	9	10	13	14	15	17	18
<i>trans</i> -CMS	3.00	6.71	7.43	7.16	6.92	7.51	7.99	3.91				
<i>cis</i> -CMS	2.93	6.55	7.13	6.58	6.39	7.39	7.99	3.89				
A-2	3.01	6.72	7.44	7.17	6.93	7.52	8.01	4.47		3.95		
A-4	3.01	6.73	7.44	7.16	6.93	7.51	7.99	4.36	1.85-1.72	3.74		
A-6	3.00	6.72	7.43	7.16	6.92	7.51	7.99	4.30	1.77-1.48	3.65		
A-8	3.00	6.73	7.45	7.15	6.93	7.52	7.99	4.31	1.75-1.36	3.64		
A-10	3.01	6.73	7.44	7.16	6.93	7.51	7.99	4.31	1.74-1.32	3.65		
M-2	3.01	6.72	7.44	7.17	6.93	7.52	7.99	4.57		4.51	6.16	5.87, 6.46
M-4	3.00	6.71	7.43	7.16	6.92	7.51	7.98	4.36	1.87-1.74	4.24	6.12	5.82, 6.41
M-6	3.00	6.72	7.43	7.15	6.92	7.51	7.98	4.32	1.80-1.49	4.17	6.12	5.81, 6.40
M-8	3.00	6.73	7.44	7.16	6.93	7.51	7.99	4.31	1.77-1.38	4.16	6.14	5.82, 6.40
M-10	3.00	6.71	7.43	7.15	6.93	7.51	7.99	4.31	1.77-1.32	4.16	6.12	5.81, 6.40
P-8	3.01	6.79	7.41	7.13	6.93	7.48	7.95	4.30	1.75-1.38	2.95		
P-10B	3.00	6.70	7.43	7.15	6.91	7.51	7.99	4.30	1.75-1.31	2.95		

* *trans*-CMS, all alcohols, monomers, and polymers had $J_{6,7} = 16.1 - 16.5$ Hz. Only *cis*-CMS had $J_{6,7} = 11.9 - 12.2$ Hz.

** NMR spectra of **P-8** and **P-10B** were measured at 90 °C with 1,1,2,2-tetrachloroethane- d_4 as solvent.

TABLE III

¹³C-NMR CHEMICAL SHIFTS IN SPECTRA OF CMS, A-n, M-n, AND P-n.

	1	2	3	4	5	6	7	8	9	10
<i>trans</i> -CMS	40.4	150.5	112.3	128.0	125.0	131.4	123.0	142.8	126.0	130.0
<i>cis</i> -CMS	40.3	149.8	111.7	129.5	124.4	132.3	125.6	143.3	128.7	130.0
A-2	40.4	150.5	112.3	128.0	124.9	131.7	122.9	143.2	125.7	130.1
A-4	40.4	150.5	112.3	128.2	125.0	131.4	123.0	142.8	125.7	129.9
A-6	40.4	150.5	112.3	128.0	125.0	131.4	123.1	142.8	125.7	129.9
A-8	40.5	150.5	112.4	128.0	125.0	131.3	123.2	142.7	125.7	129.9
A-10	40.5	150.5	112.3	128.0	125.0	131.3	123.0	142.7	125.7	129.9
M-4	40.4	150.5	112.3	127.9	125.0	131.5	123.0	142.9	125.7	129.9
M-6	40.3	150.4	112.3	128.0	124.9	131.4	123.0	142.8	125.7	129.9
M-8	40.4	150.5	112.4	128.1	125.0	131.3	123.1	142.7	125.7	129.9
M-10	40.3	150.5	112.3	128.0	125.0	131.4	123.1	142.7	125.7	129.9
P-10B	40.3	150.4	112.3	128.0	125.0	131.3	123.0	142.7	125.7	129.9

TABLE III (continued)

	11	12	13	14	15	16	17	18
<i>trans</i> -CMS	127.8	167.0	52.0					
<i>cis</i> -CMS	128.0	167.1	52.0					
A-2	128.0	166.9	66.6		61.6			
A-4	128.2	166.6	66.6	29.3 - 25.3	62.5			
A-6	128.2	166.6	64.8	32.6 - 25.4	62.9			
A-8	128.2	166.9	64.9	32.8 - 25.9	63.0			
A-10	128.1	166.6	65.0	32.8 - 25.7	63.1			
M-4	128.1	166.5	64.3	25.5 - 25.6	64.1	166.4	128.1	130.7
M-6	128.0	166.6	64.7	28.6 - 25.7	64.5	166.4	128.5	130.5
M-8	128.2	166.6	64.9	29.2 - 25.9	64.7	166.4	128.2	130.5
M-10	128.1	166.6	65.0	29.4 - 25.9	64.7	166.4	128.7	130.4
P-10B	128.2	166.6	65.0	29.5 - 25.9	a	166.6	a	a

a not observed.

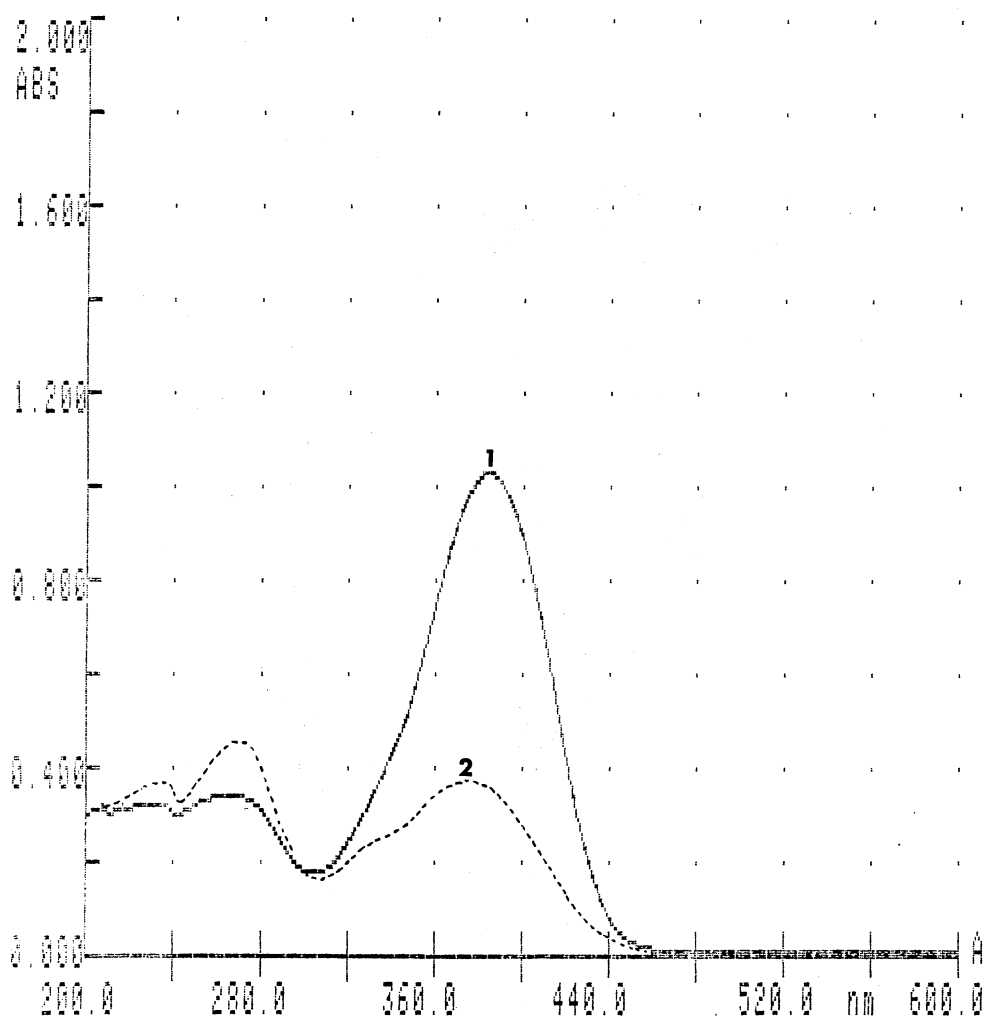


Figure 4. UV-vis absorption spectra of *trans*-CMS and *cis*-CMS

1: *trans*-CMS (2.87×10^{-5} M in chloroform).

2: *cis*-CMS (2.63×10^{-5} M in chloroform)

TABLE IV
UV-VIS SPECTRAL DATA

Compound	Solvent	$\lambda_{\max}(\text{nm})$	$\epsilon \times 10^{-4} (\text{L mol}^{-1} \text{cm}^{-1})$
<i>trans</i> -CMS	hexane	372	
	methanol	380	
	chloroform	384	3.57
<i>cis</i> -CMS	chloroform	375	1.37
A-10	chloroform	384	4.59
M-10	chloroform	384	3.84
P-10	chloroform	384	2.02

TABLE V

CHARACTERIZATION OF CMS, A-n, AND M-n.

	Yield(%)		DSC (Heating)				Elemental analysis		
	T_m °C	ΔH kcal/mol (cal/g)	T_i °C	ΔH kcal/mol (cal/g)		%C	%H	% N	
<i>trans</i> -CMS	78.0	229	8.78 (31.2)			Calcd	76.84	6.81	4.98
						Found	76.96	6.82	4.92
A-2	69.0	216	5.14 (23.3)						
A-4	74.3	191	5.09 (15.0)						
A-6	68.8	170	5.07 (13.8)						
A-8	64.6	159	4.94 (12.5)			Calcd.	75.91	8.41	3.54
						Found	76.02	8.47	3.43
A-10	60.8	149	5.00 (11.8)			Calcd.	76.56	8.81	3.31
						Found	76.66	8.85	3.32
M-2	49.2	178	3.76 (10.3)	196	0.04 (0.1)				
M-4	33.7	153	3.42 (8.7)	181	0.43 (1.1)				
M-6	72.4	142	3.79 (9.0)	175	0.55 (1.3)				
M-8	85.6	133	3.96 (8.8)	166	0.22 (0.5)	Calcd.	74.80	7.85	3.12
						Found	74.65	7.85	3.08
M-10	89.5	126	3.87 (8.1)	159	0.29 (0.6)	Calcd.	75.44	8.23	2.91
						Found	75.37	8.24	2.91

TABLE VI

CHARACTERIZATION OF POLYMERS

	Yield(%)	GPC			DSC (Heating)			Elemental analysis			
		$M_w \times 10^{-3}$	$M_n \times 10^{-3}$	M_w/M_n	T_g °C	T_i °C	ΔH kcal/mol(cal/g)	%C	%H	%N	
P-2	48	14.3	5.7	2.5	129	139	0.09 (0.25)				
P-4	20	7.1	2.8	2.5	119	130	0.28 (0.72)				
P-6	26	9.7	3.9	2.5	109	125	0.41 (0.98)				
P-8	24	9.1	3.4	2.7	91	121	0.52 (1.16)				
P-8B	31	27.6	11.0	2.5	96	130	0.18 (0.41)	Calcd.	74.80	7.85	3.12
								Found	74.54	7.93	3.24
P-10	27	10.3	5.2	2.0	81	117	0.58 (1.21)				
P-10B	41	36.9	10.9	3.4	83	125	0.43 (0.89)	Calcd.	75.44	8.23	2.93
								Found	75.45	7.97	2.99

CHAPTER III

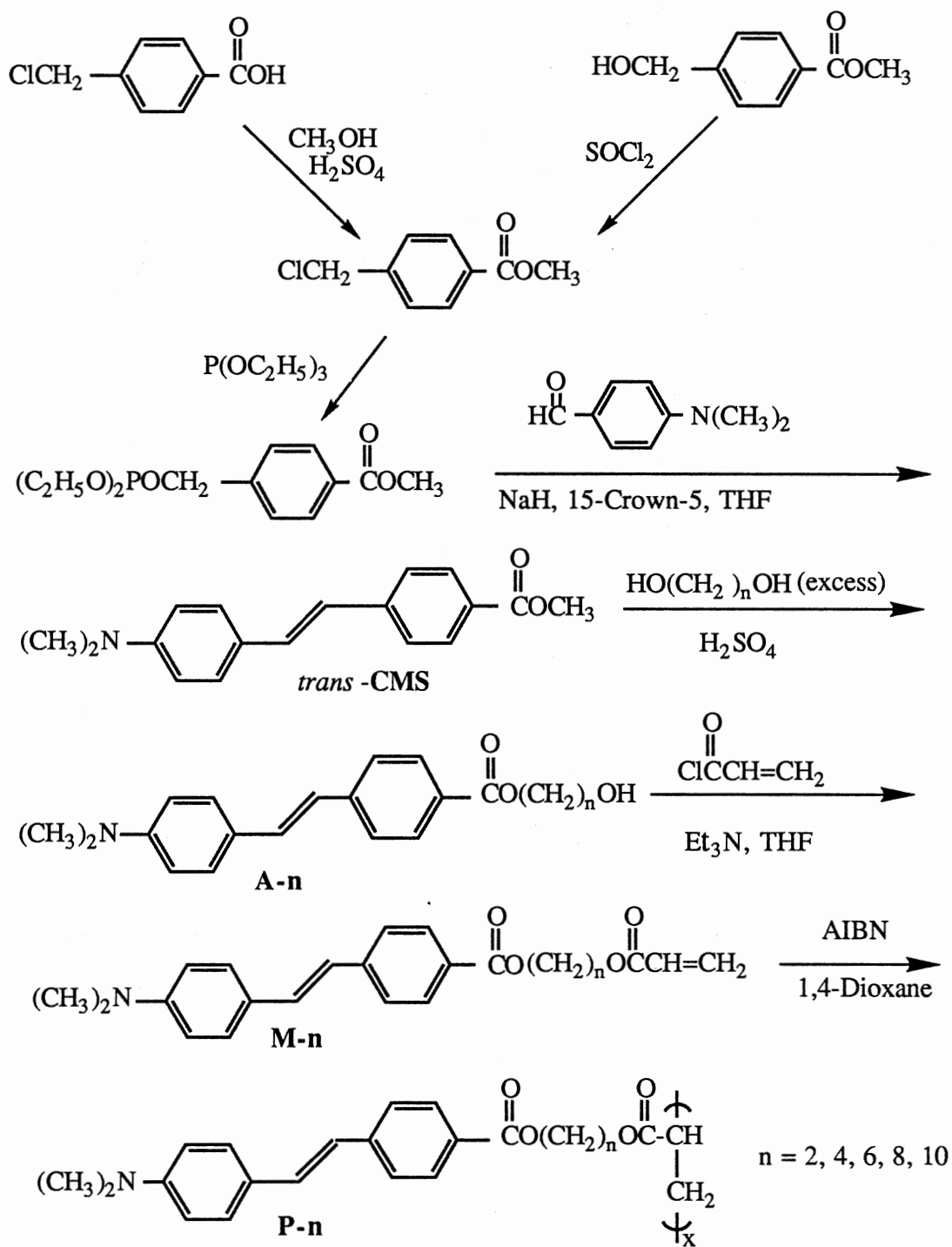
RESULTS

Syntheses. The monomers and polymers were synthesized as shown in Scheme I.

A number of methods have been reported for the synthesis of unsymmetrically substituted stilbenes.²⁹ The Wittig reaction is the most popular method. One limitation of the classic Wittig reaction is that the stilbenes usually are formed as a mixture of *trans*- and *cis*-isomers together with triphenylphosphine oxide. A difficult separation may give a lower yield. The first synthesis of 4-carbomethoxy-4'-(*N,N*-dimethylamino)-*trans*-stilbene (*trans*-CMS) was reported by G. P. Schiemenz and M. Finzenhagen in 1981.²⁷ They found that *trans*-CMS cannot be prepared directly by a Wittig reaction, and they prepared *trans*-CMS in 26% yield by acidic hydrolysis of 4-cyano-4'-(*N,N*-dimethylamino)-*trans*-stilbene, which was synthesized by a Wittig reaction. Therefore in this work an alternative synthetic method was used. The new method is based on the Wadsworth-Emmons modification of the Wittig reaction using a crown ether.³⁰ The crown ether has the ability to solvate the cations, and the resulting unencumbered anions are more reactive nucleophiles. In this experiment it was confirmed that the addition of a catalytic quantity of 15-crown-5 ether greatly facilitates the reaction. The pure *trans*-CMS was obtained in a yield of 78%.

The ¹H NMR spectra of all stilbene compounds prepared in this investigation are reported in Table II, and the ¹³C NMR spectra are in Table III.

Scheme I



In an early experiment it was found that both the color and the ^1H NMR spectrum of a CMS solution in CDCl_3 changed when exposed to laboratory fluorescent light for a long time. We speculated that the CMS may undergo photoisomerization. This idea was confirmed, as *cis*-isomer was separated from the mixture solution. The *trans*- and *cis*-isomers of CMS can be distinguished conveniently by ^1H NMR. The *trans*-CMS showed its ethylenic protons at δ 6.92 and 7.16 ($J = 16.2\text{-}16.4$ Hz). The *cis*-CMS showed its ethylenic protons at δ 6.39 and 6.58 ($J = 11.9\text{-}12.2$ Hz). The isomer ratio of the mixture can be determined from ^1H NMR spectra by comparing the relative intensities of the signals arising from the dimethylamino groups, for *trans*-CMS at δ 3.00, and for *cis*-CMS at δ 2.93.

The structures of the *trans*- and *cis*-isomers were also confirmed by their UV-visible spectra. The *trans*-isomer showed a maximum at 384 nm with a stronger intensity and *cis*-isomer absorbed at 375 nm with a weaker intensity. UV-visible spectra and data for different compounds are shown in the Figure 4 and Table IV. The UV-vis data show that the chromophore is not changed during the reactions that convert CMS to A-10 to M-10 to P-10.

Liquid Crystal Properties of Alcohols A-n and Monomers M-n.

Synthetic yields, elemental analyses, and DSC transition temperatures and enthalpies of the intermediates alcohols A-n and monomers M-n are reported in Table V. Four of the alcohols A-n have only one phase transition by DSC, as shown in Figures 5, 6, 7, and 8. There was a solid-solid transition in the DSC thermograms of A-10 (Figure 9) because of crystalline polymorphism. When samples were cooled from the isotropic liquid phase, birefringent textures were observed between crossed polarizers with the microscope as shown for A-4, A-6, A-8 and A-10 in Figures 10, 11, 12 and 13. The mesomorphic phase transitions of monomers were detected with both the DSC and the polarizing microscope. All of the five acrylate monomers M-n were enantiotropic liquid crystals, as

shown in Figures 5-9 for their DSC thermograms and Figures 14-17 for their textures. Since the monomers undergo thermally induced polymerization during their characterization, it is hard to measure the transition temperatures accurately. The effect of the number of methylenic units on the mesophase behavior of the five monomers is shown in the Figure 22.

Liquid Crystal Properties of Polymers. Yields after two precipitations, elemental analyses, GPC analyses and DSC data for polymers **P-n** are reported at Table VI. All of the five polymers showed liquid crystal properties. The texture changes corresponding to the phase transitions in DSC were observed as shown in Figures 5-9 for their DSC thermograms and Figures 18-21 for their textures. The thermograms shown are from samples that were annealed about 10 h at 5-10 degrees below T_i . Some properties of the polyacrylates are similar to those of the acrylate monomers. Both T_g and T_i of these polymers decreased with increase of the length of the spacer (Figure 23).

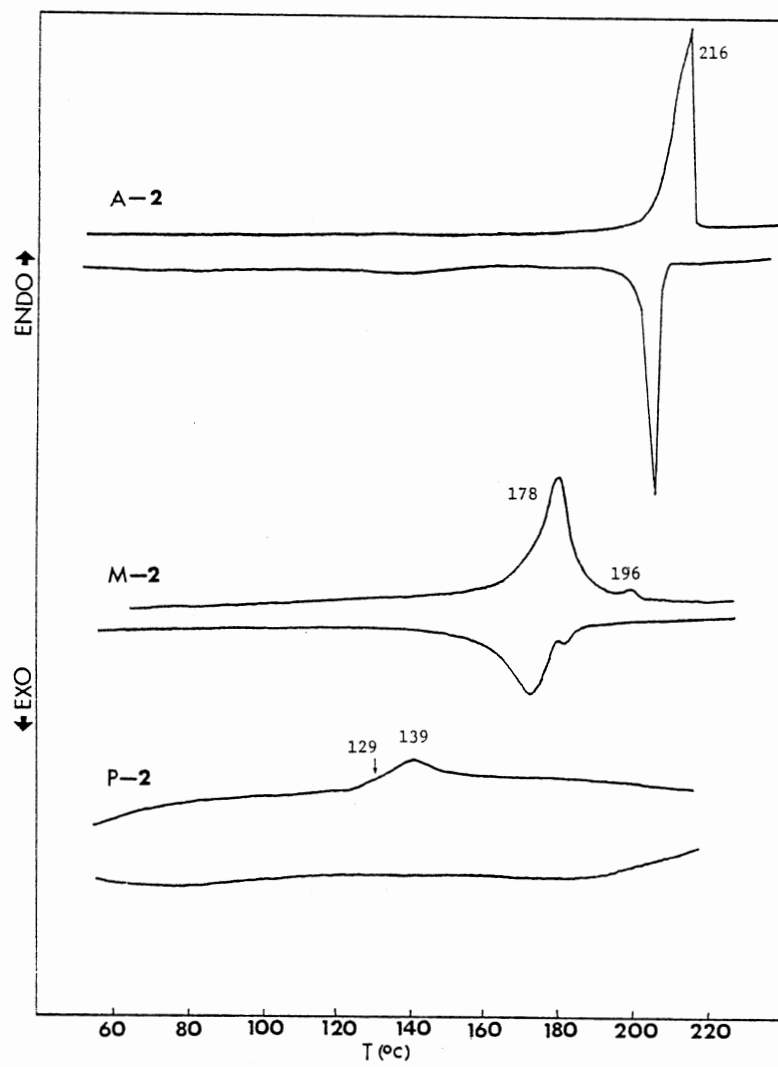


Figure 5. DSC thermograms of A-2, M-2 and P-2.

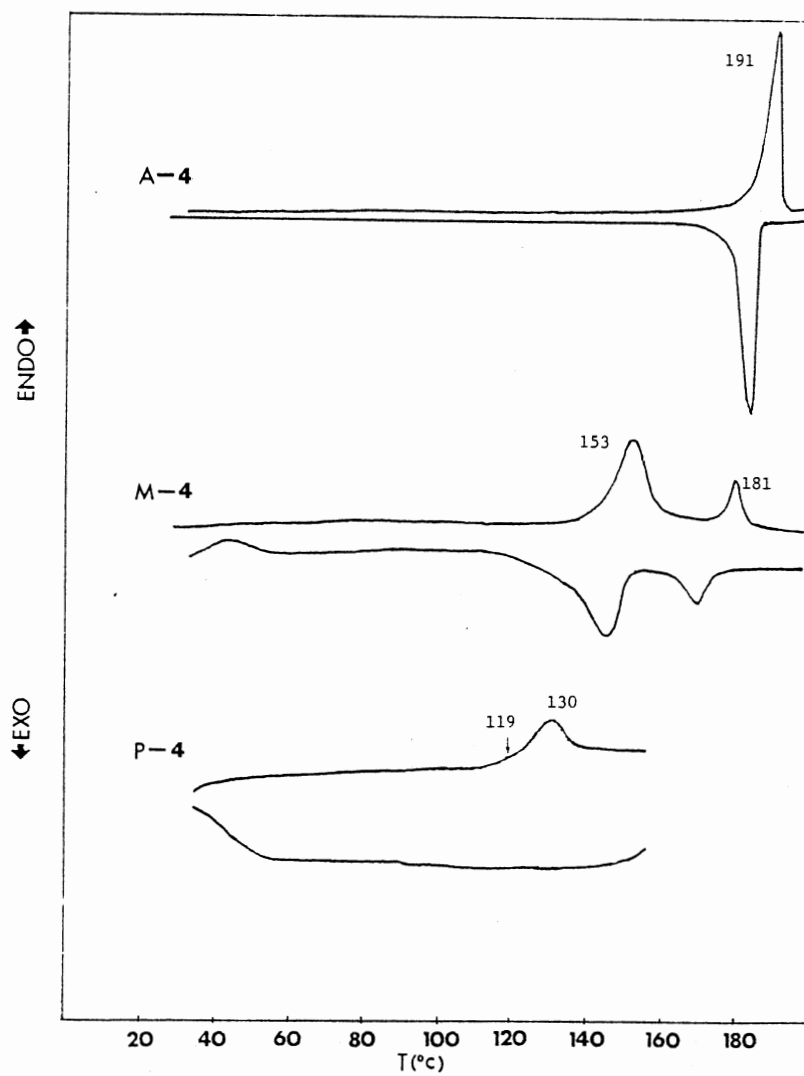


Figure 6. DSC thermograms of A-4, M-4 and P-4.

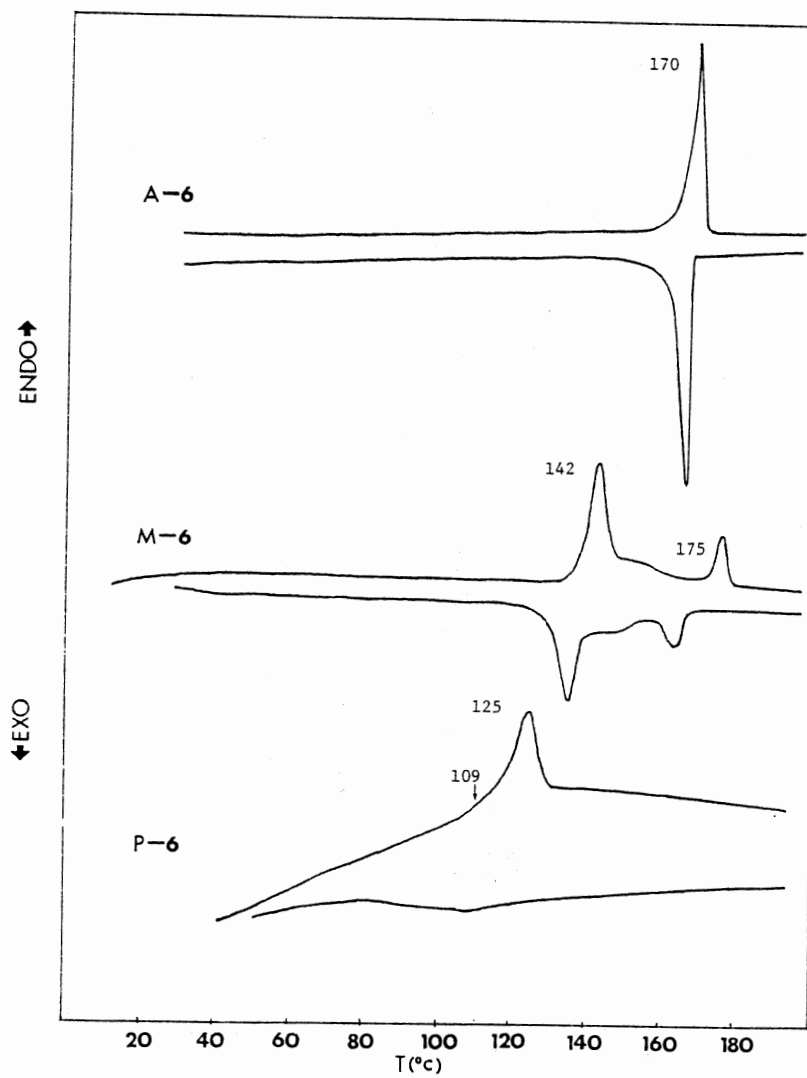


Figure 7. DSC thermograms of A-6, M-6 and P-6.

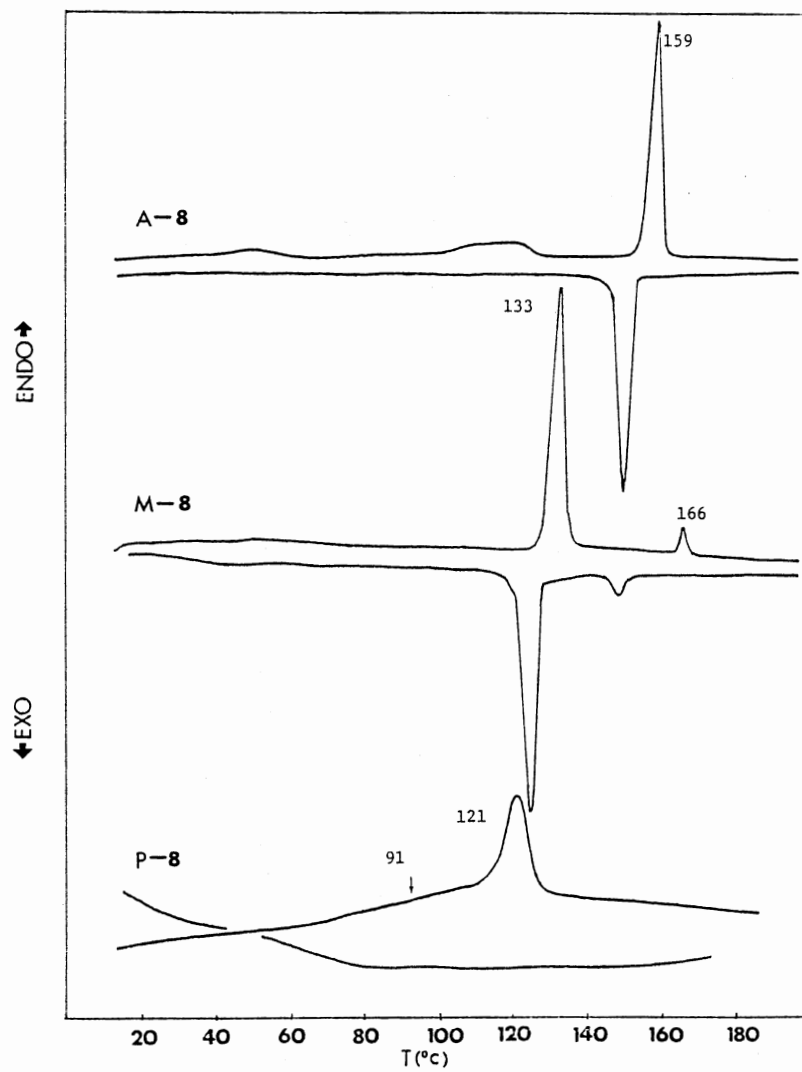


Figure 8. DSC thermograms of A-8, M-8 and P-8.

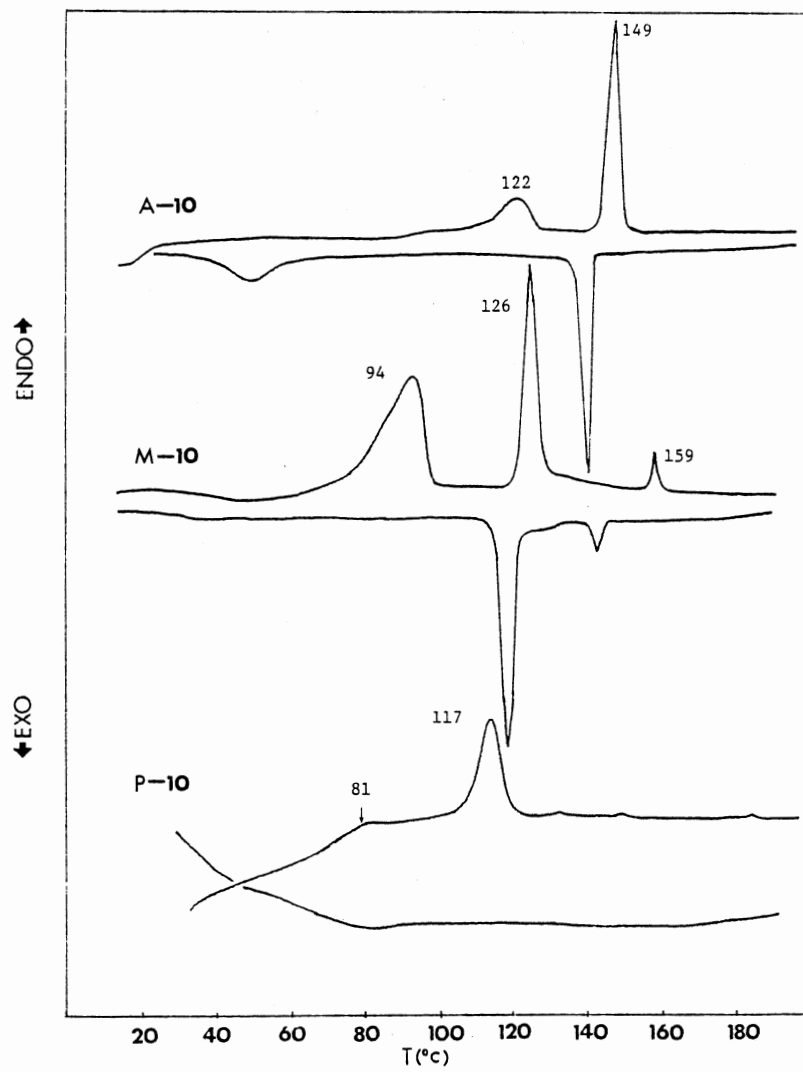


Figure 9. DSC thermograms of A-10, M-10 and P-10.

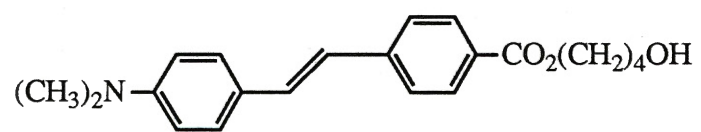
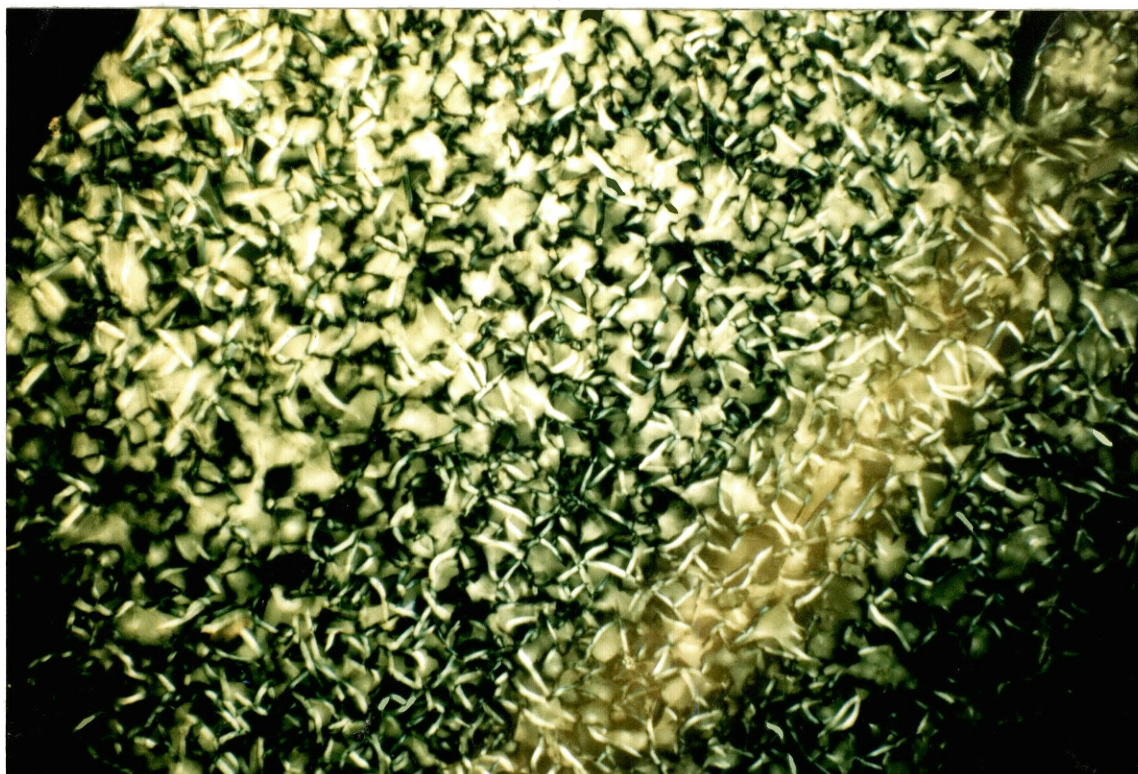


Figure 10. A-4 between crossed polarizers at 170 °C, cooling scan (50 X).

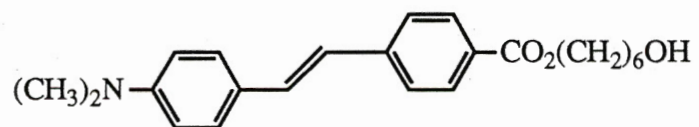


Figure 11. A-6 between crossed polarizers at 160 °C, cooling scan (50 X).

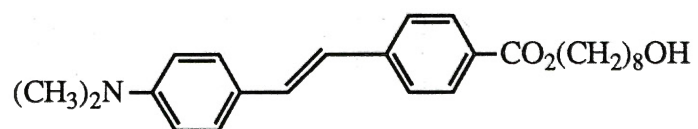
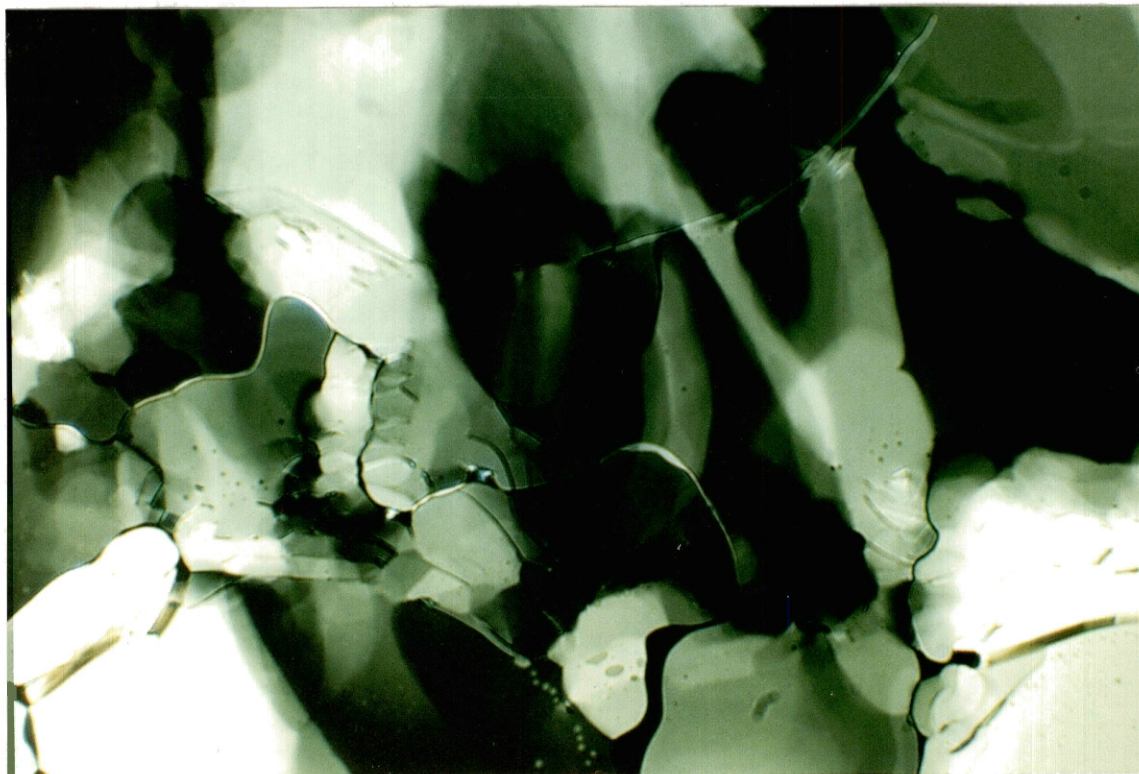


Figure 12. A-8 between crossed polarizers at 150 °C, cooling scan (200 X).

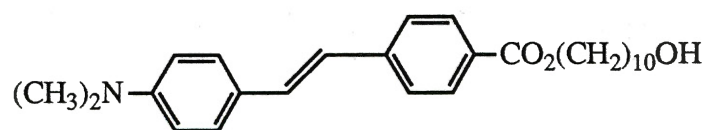
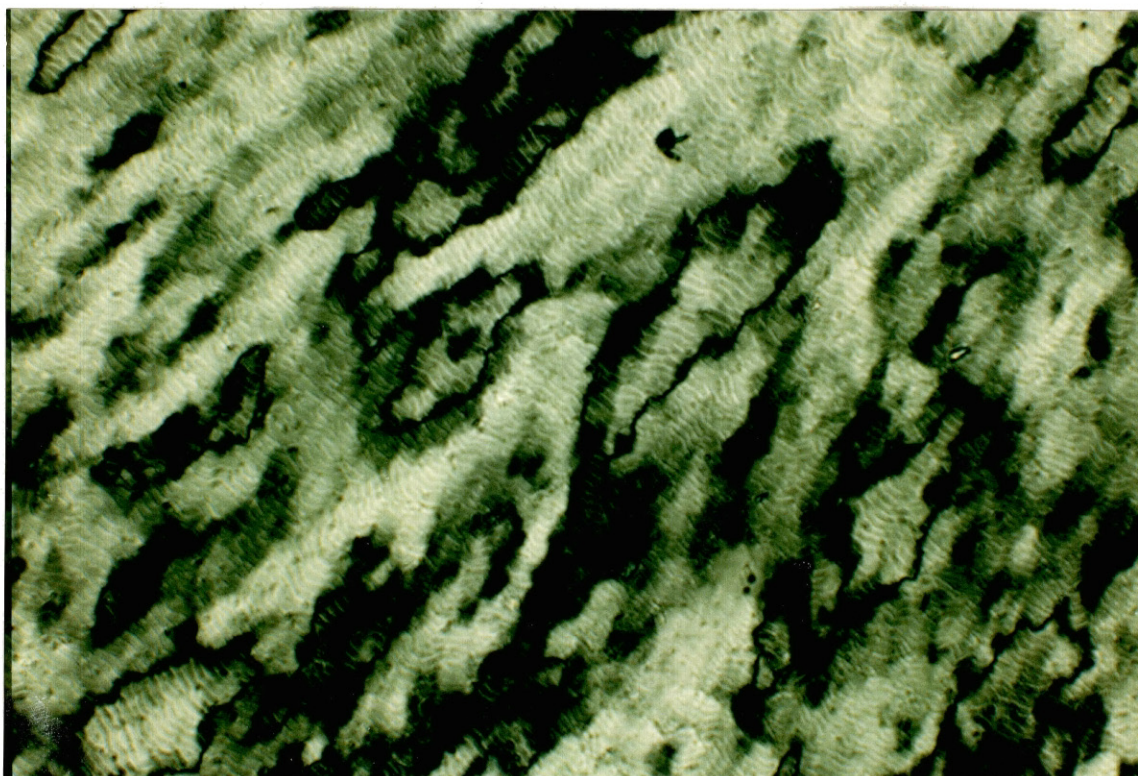


Figure 13. A-10 between crossed polarizers at 143 °C, cooling scan (50 X).

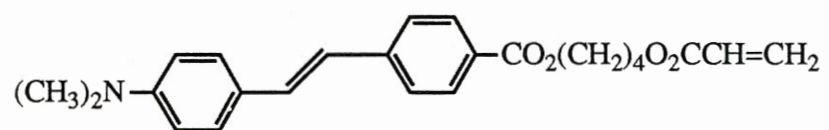
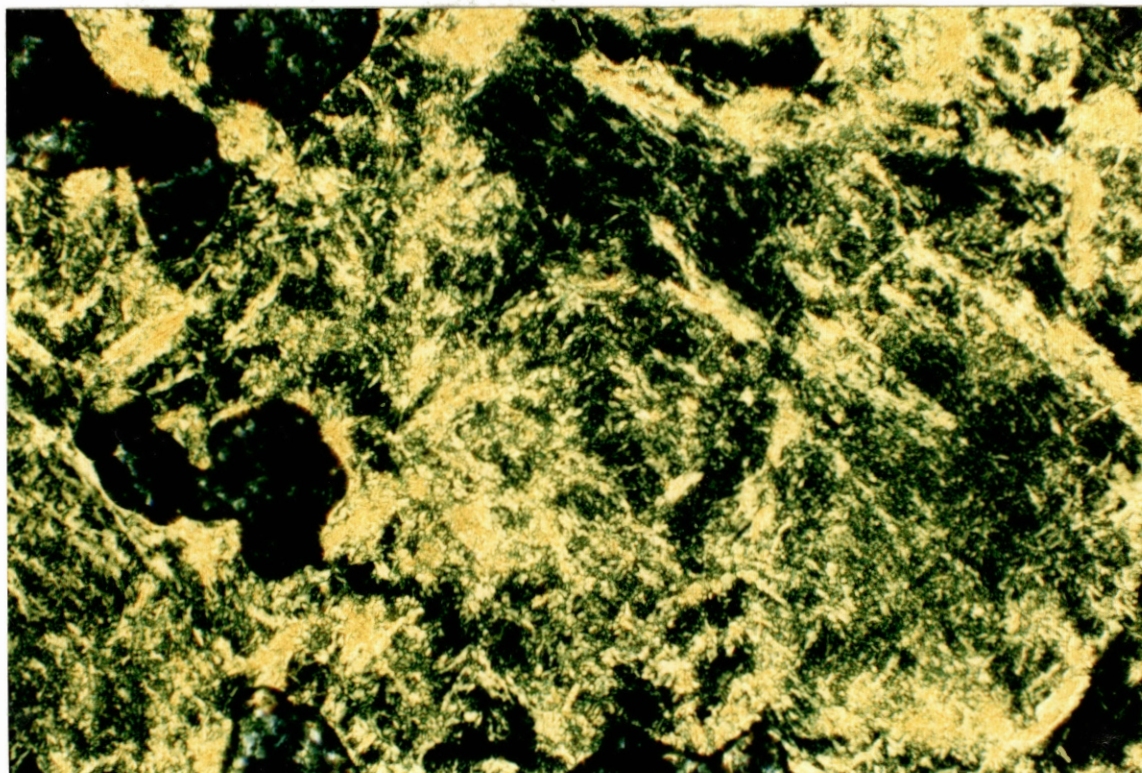


Figure 14. M-4 between crossed polarizers at 180 °C, heating scan (200 X).

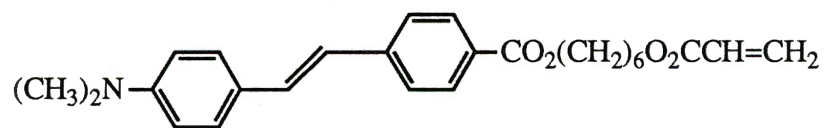


Figure 15. **M-6** between crossed polarizers at 160 °C, heating scan (200 X).

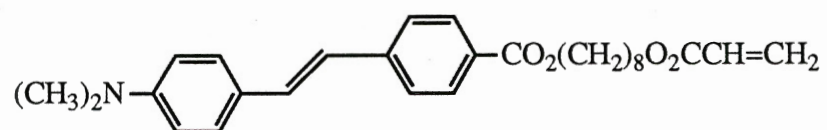
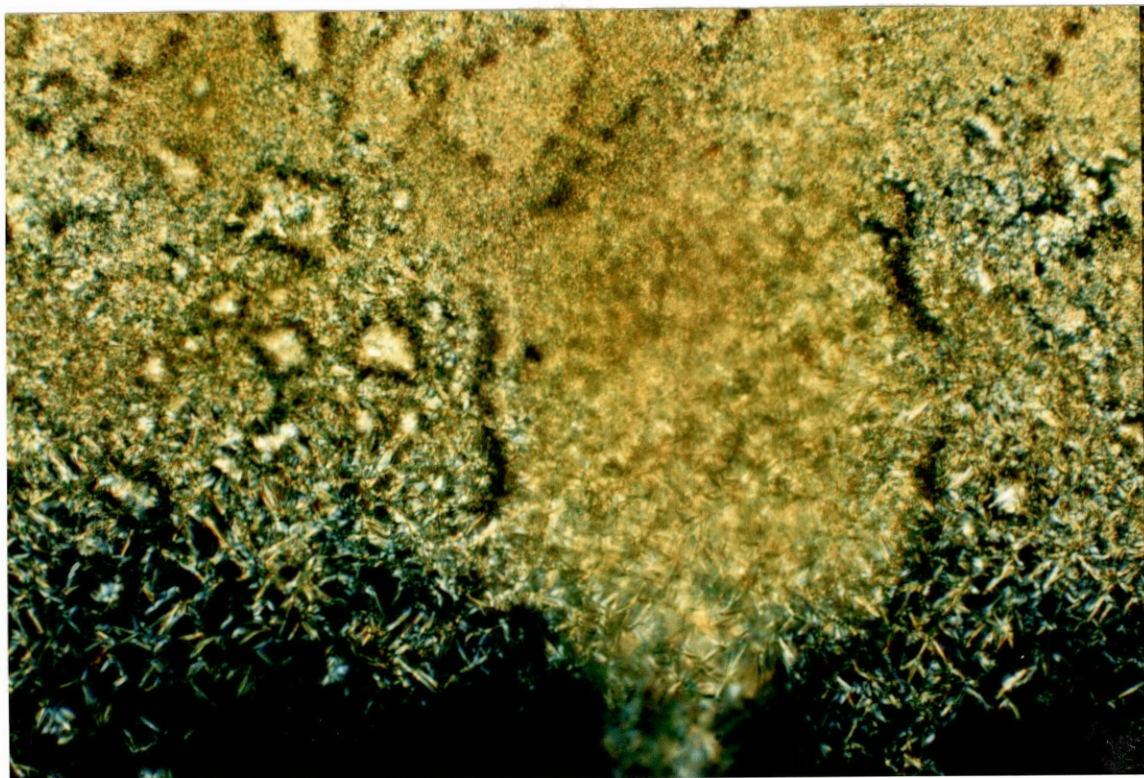


Figure 16. **M-8** between crossed polarizers at 115 °C, cooling scan (200 X).

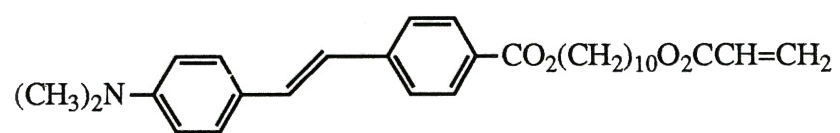
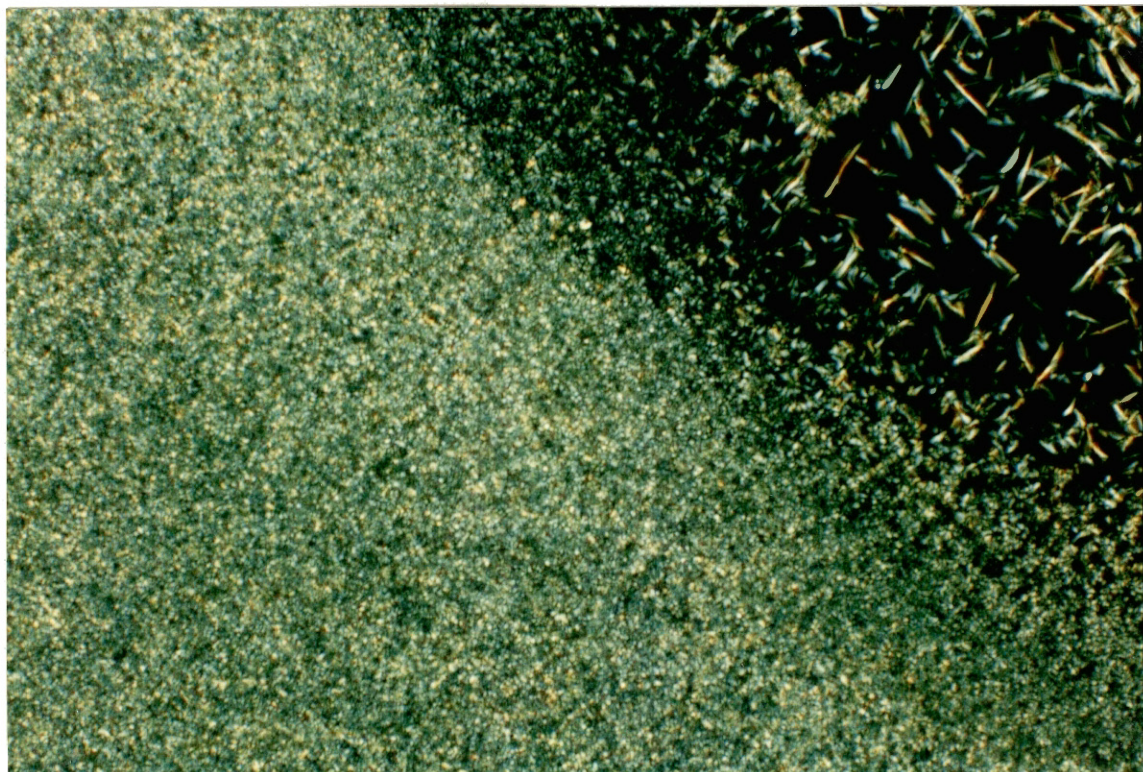


Figure 17. **M-10** between crossed polarizers at 110 °C, cooling scan (200 X).

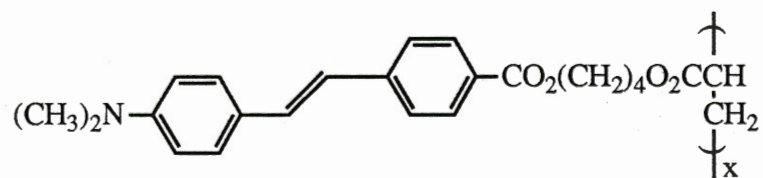
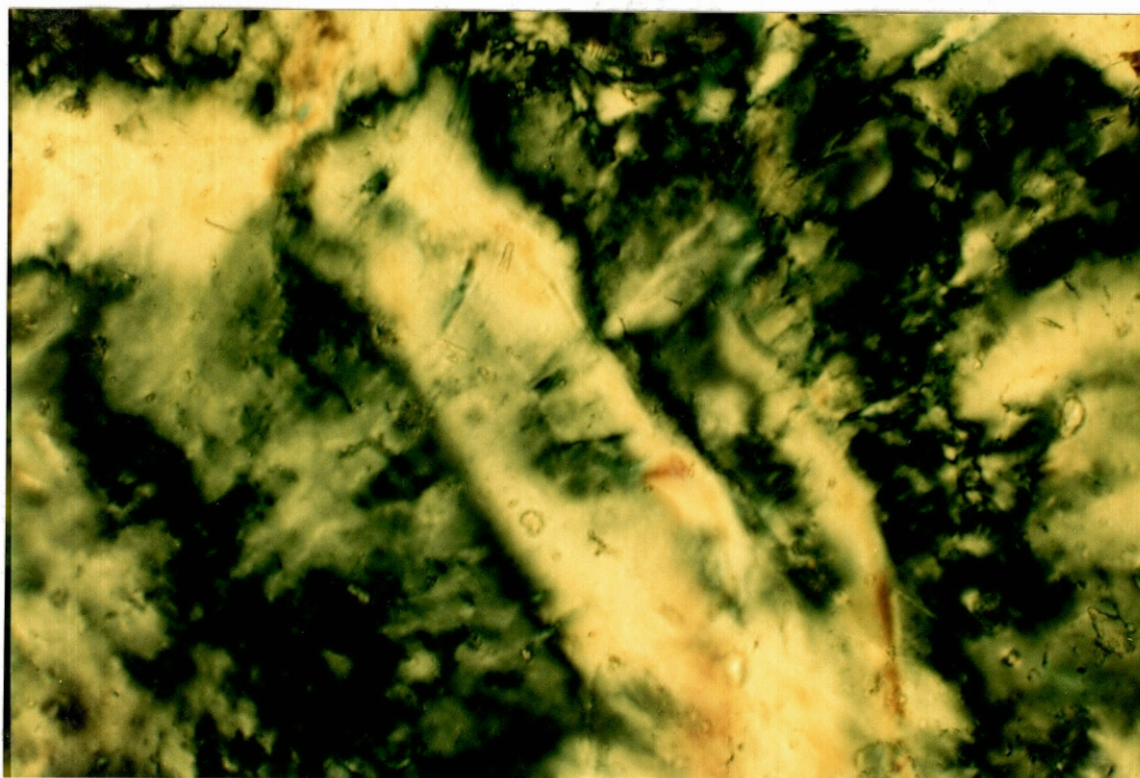


Figure 18. P-4 between crossed polarizers, annealed at 125 °C for 10 h (200 X).

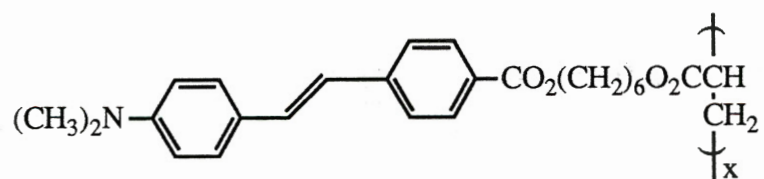
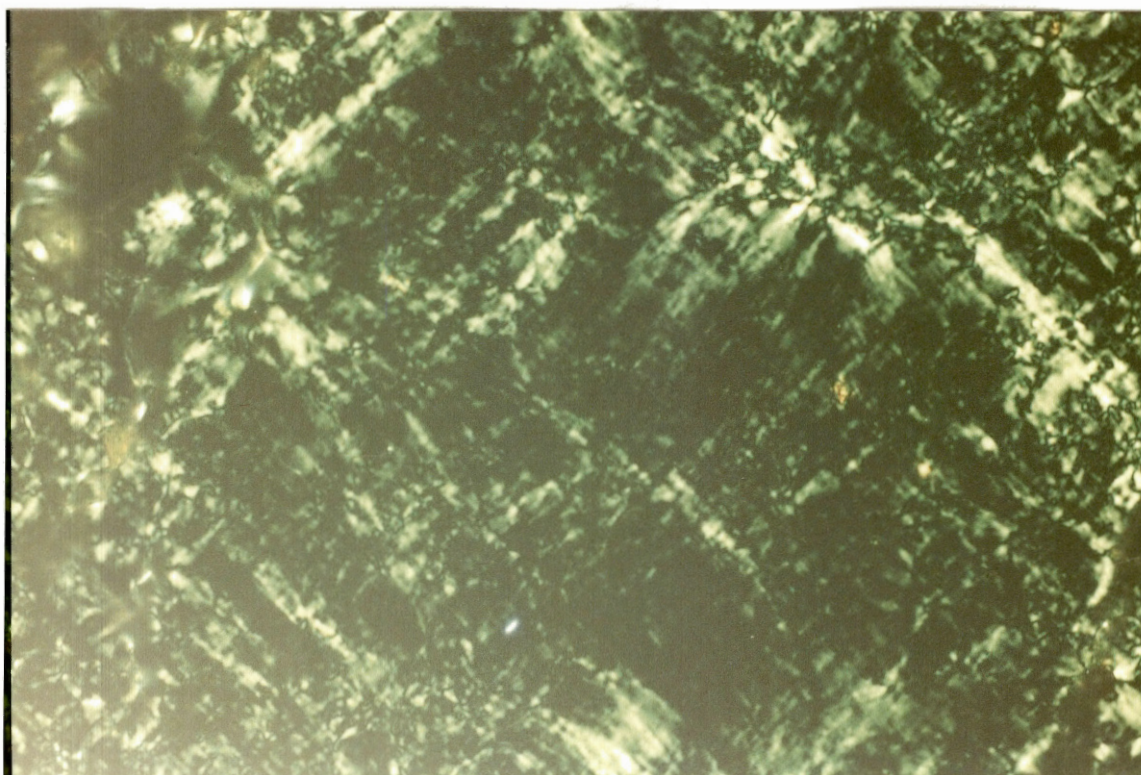


Figure 19. **P-6** between crossed polarizers at 131 °C, heating scan (400 X).

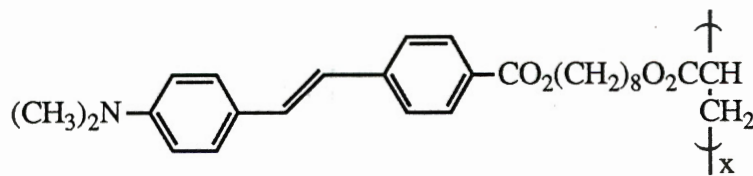
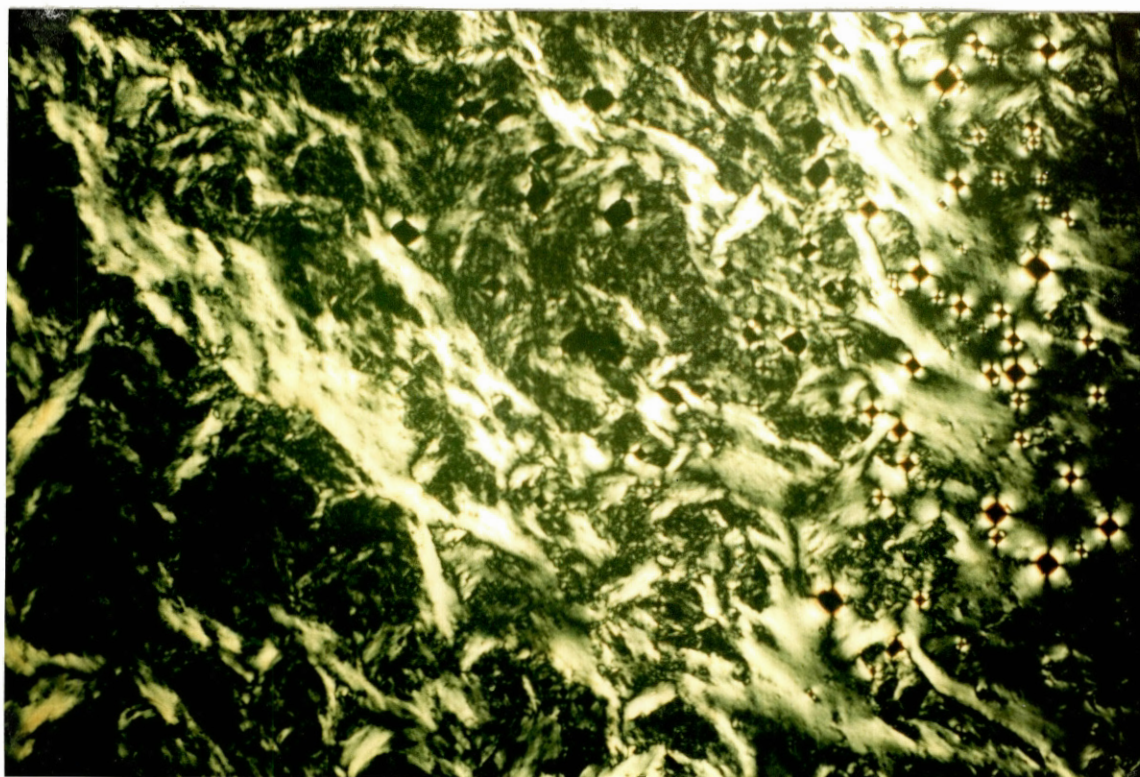


Figure 20. **P-8** between crossed polarizers, annealed at 105 °C for 12 h (50 X).

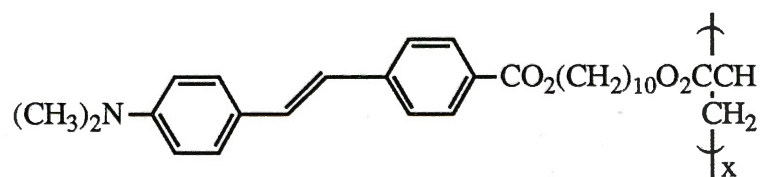
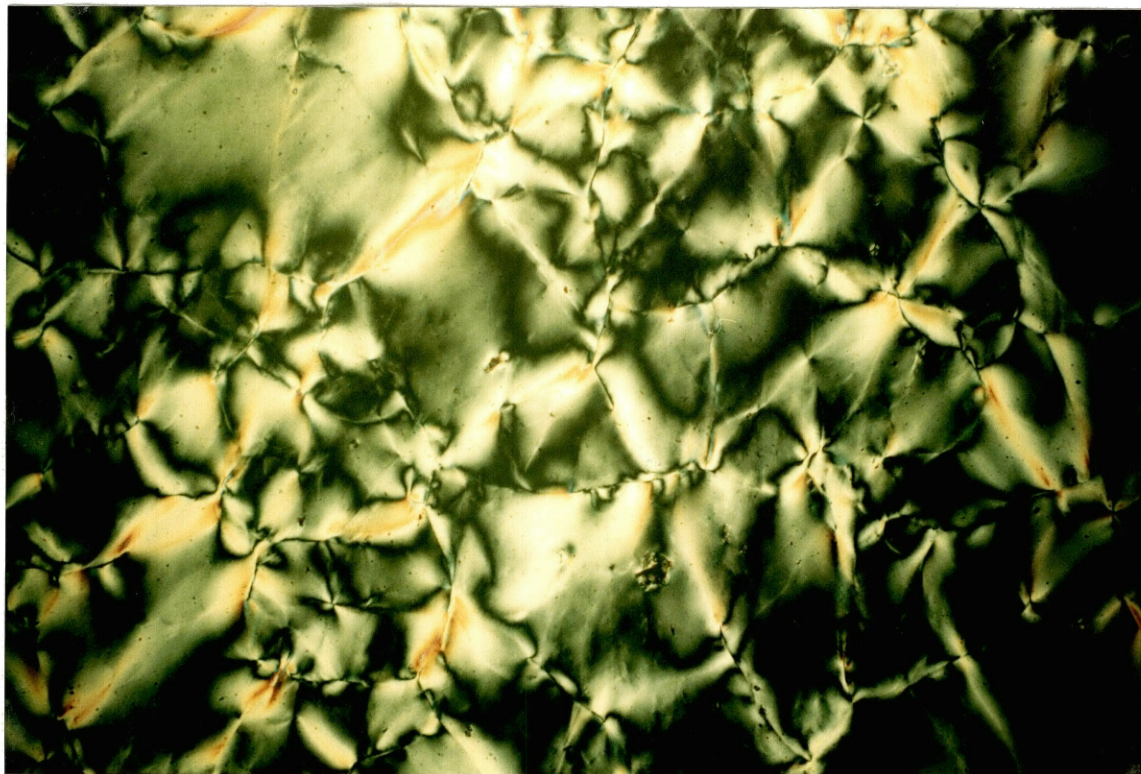


Figure 21. P-10 between crossed polarizers, annealed at 108 °C for 10 h (50 X).

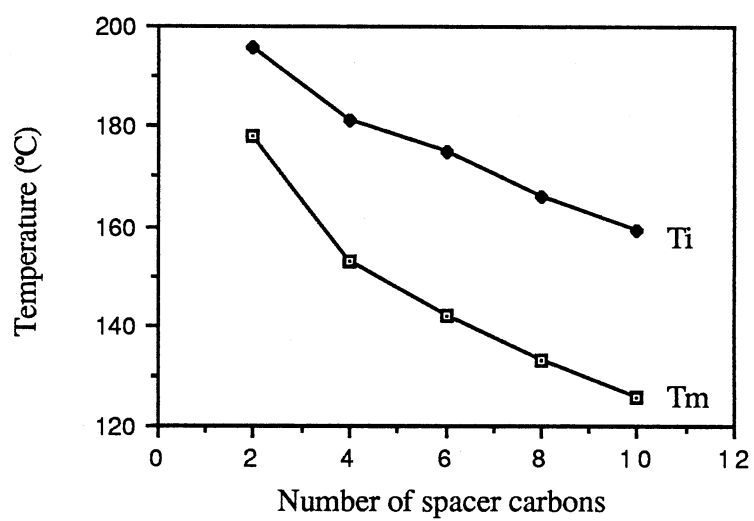


Figure 22. Dependence of melting and isotropic transition temperatures of monomers **M-n** on spacer length.

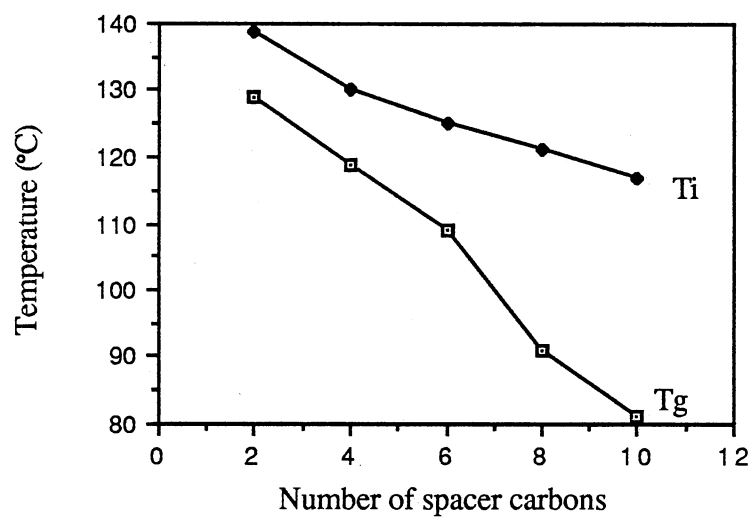


Figure 23. Dependence of glass and isotropic transition temperature of polymers on carbon spacer length.

Some liquid crystal behavior of the polymers was different from that of the monomers. In the monomers DSC thermograms the melting and isotropization transitions were clearly observed in both heating and cooling scans at 20 °C/min. In the polymer DSC thermograms the T_g and T_i transitions were observed in the heating scans, but in the cooling scans only the T_g was observed. By polarizing microscopy, when the isotropic polymer melt was cooled from the isotropic phase at a rate of 0.1 °C/min, the nematic texture slowly reappeared. To get the clear textures the polymer samples had to be kept 5-10 °C below T_i for several hours. Apparently liquid crystalline order develops very slowly in these polymers. This conclusion also is supported by DSC annealing experiments. The DSC thermograms of the same polymer sample (**P-8B**) with different thermal histories are given in Figure 24. After the first heating and cooling scans, when the polymer sample was heated again without annealing, only the glass transition appeared in the second heating and cooling scans. Annealing of **P-8B** at 100 °C for more than 24 h before repetition of the thermogram revealed the isotropic transition again at about 130 °C. To get clear and reproducible DSC thermograms the polymer samples should be near an equilibrium state. The polymers with short 2, 4, and 6-carbon spacers required longer annealing to obtain clear and reproducible thermograms.

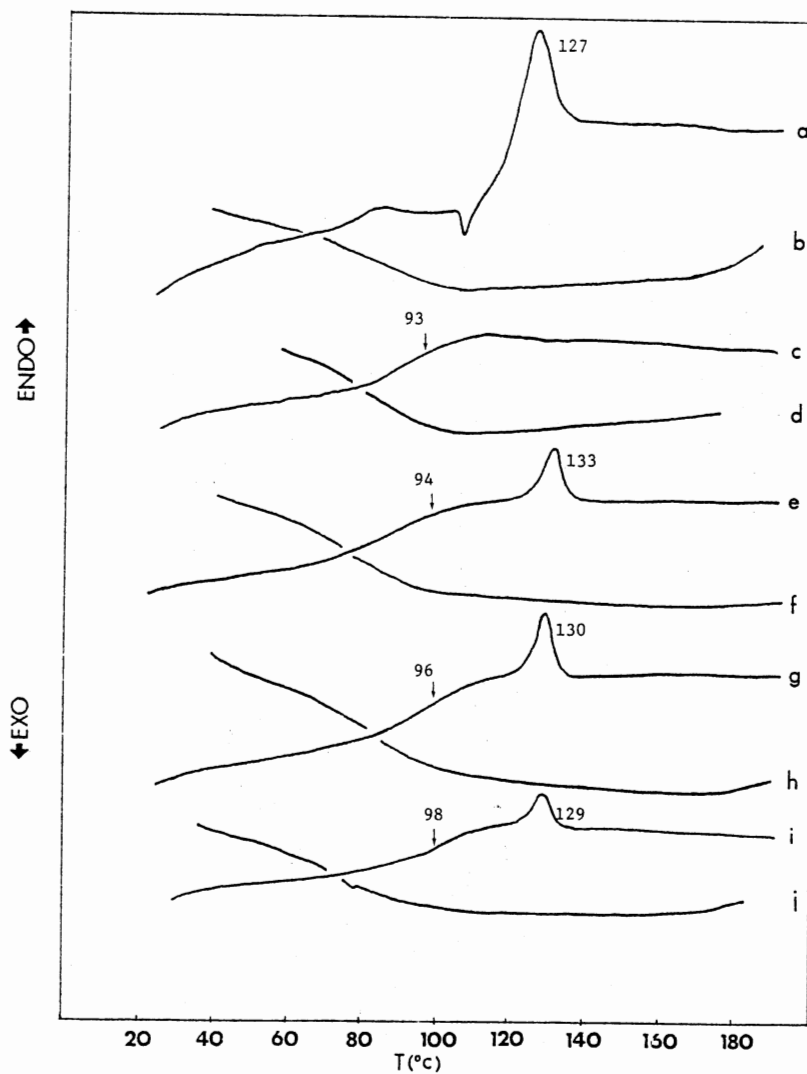


Figure 24. Repeated DSC analyses of **P-8B**.

a: First heating scan ($\Delta H_i = 1.45$ cal/g). b: First cooling scan, after 2 min at 180 °C. c: 2nd heating scan, after 5 min at 25 °C. d: 2nd cooling scan; 2 min at 180 °C. e: 3rd heating scan; 26 h at 100 °C and cooled to 25 °C ($\Delta H_i = 0.38$ cal/g). f: 3rd cooling scan; 2 min at 180 °C. g: 4th heating scan, 60 h at 100 °C and cooled to 25 °C ($\Delta H_i = 0.45$ cal/g). h: 4th cooling scan; 2 min at 180 °C. i: 5th heating scan; 100 h at 100 °C and cooled to 25 °C ($\Delta H_i = 0.29$ cal/g). j: 5th cooling scan; 2 min at 180 °C.

Polymer Film Making. Spin-coating is the best method for obtaining a thin (0.2-2 μm), uniform, adherent, homogeneous polymer film.^{31, 32} It is accomplished by dropping a polymer solution onto the substrate that rotates at a constant speed (1000-8000 rpm). Evaporation of the solvent from the spinning substrate leaves a polymer film. The film thickness is related to the evaporation rate, the latent heat of evaporation, the heat capacity of the solvent, the viscosity of the solution and the angular velocity. Experimental results at different rotating speeds are given in Table VII. For each film 40-60 drops of polymer solution were used, and each drop was about 0.04 mL. For a given polymer solution and a given piece of equipment, the thickness of the polymer film depends on the spinning speed. So it is convenient to control the thickness of the polymer film by using different spinning speeds.

TABLE VII

RELATION OF THICKNESS AND SPINNING SPEED FROM
SPIN-COATING OF 10% P-10B IN 1,4-DIOXANE

Spinning speed (rpm):	700	750	1000	1500	2000	2500
Thickness (μm):	1.85	1.81	1.73	1.56	1.39	0.95

CHAPTER IV

DISCUSSION

All of the five polyacrylates exhibited nematic liquid crystal properties. By polarizing microscopy they showed nematic schlieren textures and singularities with both two and four associated brushes. The low values of their isotropization enthalpies in DSC thermograms are also evidence for nematic phases. Isotropization enthalpies of 0.1-0.6 kcal/mol suggest a low degree of order. Generally a highly ordered mesogenic phase shows a greater isotropization enthalpy. The greater order of the smectic state (S_C or S_A) usually gives a greater ΔH_i of the smectic-isotropic transition (about 0.7-1.5 kcal/mol) compared with that of the corresponding nematic-isotropic transition (about 0.1-0.5 kcal/mol).³

Figure 25 shows that the molar isotropization enthalpies of the polymers increase with increasing the number of spacer carbons, but even with ten spacer carbons ΔH_i was only 0.58 kcal/mol. A longer spacer leads to a more ordered mesophase. It is possible to get different liquid crystalline phases by changing the length of the spacer.⁷

The phase transition temperatures of the polymers and monomers were mainly determined by the highly polar NLO/LC side chain group. The higher transition temperatures approximately were linearly related to the mass fraction of the polar core (Figure 26). It is predicted that if the mass fraction of NLO/LC unit is further decreased by use of a longer alkyl chain as the spacer, the polymer will show a broader and lower mesogenic temperature range, and perhaps a smectic phase.

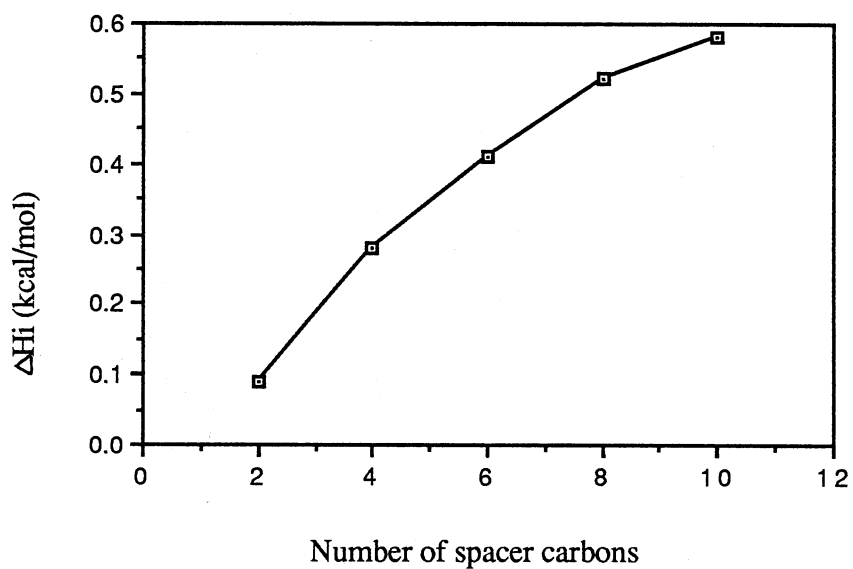


Figure 25. Dependence of molar isotropization enthalpies of polymers on the number of spacer carbons. Data are from samples **P-2**, **P-4**, **P-6**, **P-8** and **P-10** (Table VI).

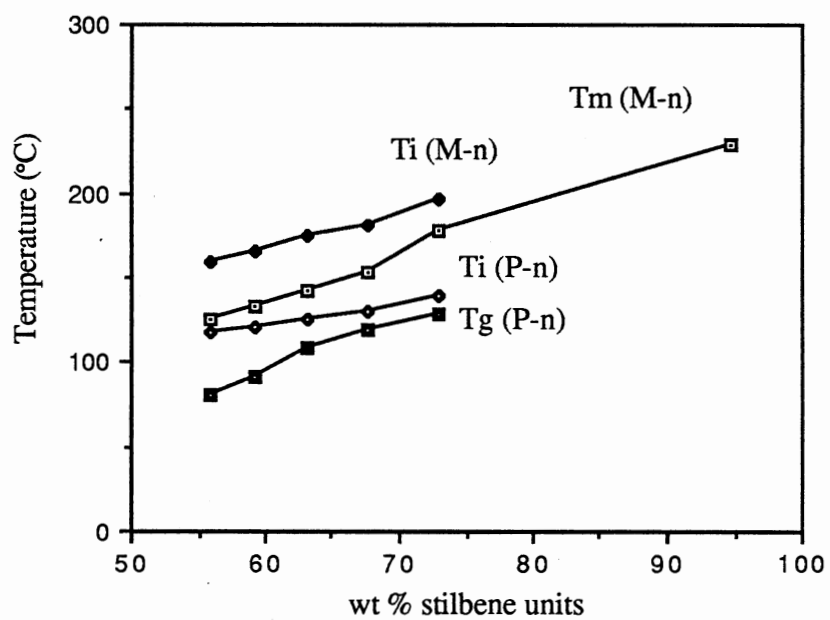


Figure 26. Dependence of phase transition temperatures on mass fraction of polar core.

For liquid crystalline polymers the mesomorphic transitions also depend on molecular weight, M_n . As molecular weight or degree of polymerization, DP_n , increases, the transition temperature increases up to a certain molecular weight and then levels off.³³ For some side chain LCPs the most drastic effect of the degree of polymerization on the phase transition temperature was observed for $DP_n < 10$. The degree of polymerization of **P-2**, **P-4**, **P-6**, **P-8** and **P-10** was from 7.2 to 15.7. The phase transition temperatures may still depend on the molecular weight of the polymer. If molecular weight is increased, the phase transitions will shift to higher temperatures. The DP_n of **P-8B** and **P-10B** are 24.7 and 22.7, above the limit where molecular weight influences the mesomorphic transition. Their higher molecular weights lead to higher glass and isotropic transition temperatures than those of **P-8** and **P-10**.

The thermal properties of liquid crystalline polymer may be affected by the purity of the polymer. The presence of the very small amounts of residual monomer will reduce both glass and isotropic transition temperatures.³⁴ In this work the purity of the polymers was monitored by GPC analyses. There were no detectable residual monomers in the polymer samples.

For comparison the phase behaviors of new polymer (**P-6**) and the related side chain polyacrylates from the literature are presented in the Table VIII. The comparison leads to the conclusion that new side chain polymers containing a highly polar stilbene show higher glass transition temperatures than those of side chain polymers containing only biphenyl, phenyl ester, and less polar stilbene units. The glass transition corresponds to the onset of long range molecular motion of the polymer. The mass of the bulky mesogenic unit and very strong dipole-dipole interactions, which come from the highly polarizable stilbene, reduce the mobility of the mesogenic side chains of the polymer and cause a higher glass transition temperature. For NLO and other applications, a T_g well above room temperature may be advantageous, because it favors a long time stability of the

oriented state at room temperature. Some samples of NLO compounds dissolved in polymer glasses and side chain polymers with lower T_g 's lose their order during periods of hours or days while standing at room temperature.^{40, 41}

It was hard to identify the mesophases of the monomers by polarizing microscopy. However, the low values of isotropization enthalpies from the DSC thermograms suggest less ordered nematic mesomorphism of these monomers. Since it is not reliable to assign the mesophase based only DSC data, the assignments of nematic mesophases need to be verified by X-ray analyses or other methods.

The acrylate monomers show higher melting points than most previous acrylates containing LC units, which are compiled in Table IX. The highly polarizable 4-(N,N-dimethylamino)stilbene-4'-carboxylate group leads to very strong intermolecular dipole-dipole interactions, which restrict the freedom of motion of the side chain and favor the formation of higher melting crystals. The higher melting points of new acrylates are responsible for the decrement of the mesogenic temperature range.

TABLE VIII
COMPARISON OF POLYACRYLATES

$\left(\text{CH}_2 - \underset{\substack{\text{C}=\text{O} \\ \text{O}-(\text{CH}_2)_6-\text{O}-\text{Y}}}{\text{CH}} \right)_x$	Phase Transition (°C)	Reference
$\text{Y} = \text{---} \text{C}(=\text{O}) \text{---} \text{C}_6\text{H}_4 \text{---} \text{CH}=\text{CH} \text{---} \text{C}_6\text{H}_4 \text{---} \text{N}(\text{CH}_3)_2$	G 109 N 125 I	
$\text{Y} = \text{---} \text{C}_6\text{H}_4 \text{---} \text{C}(=\text{O}) \text{---} \text{C}_6\text{H}_4 \text{---} \text{OCH}_3$	G 35 S 97 N 123 I	35
$\text{Y} = \text{---} \text{C}_6\text{H}_4 \text{---} \text{C}(=\text{O}) \text{---} \text{C}_6\text{H}_4 \text{---} \text{OC}_4\text{H}_9$	G 30 LC1 103 LC2 114 I	36
$\text{Y} = \text{---} \text{C}_6\text{H}_4 \text{---} \text{C}(=\text{O}) \text{---} \text{C}_6\text{H}_4 \text{---} \text{CN}$	G 33 N 133 I	37
$\text{Y} = \text{---} \text{C}_6\text{H}_4 \text{---} \text{C}(=\text{O}) \text{---} \text{C}_6\text{H}_4 \text{---} \text{OC}_6\text{H}_{13}$	G 28 S 130 I	37
$\text{Y} = \text{---} \text{C}_6\text{H}_4 \text{---} \text{C}(=\text{O}) \text{---} \text{C}_6\text{H}_4 \text{---} \text{N}=\text{CH} \text{---} \text{C}_6\text{H}_4 \text{---} \text{CN}$	G 35 N 211 I	37
$\text{Y} = \text{---} \text{C}_6\text{H}_4 \text{---} \text{C}_6\text{H}_5$	G 48 K 57 I	38
$\text{Y} = \text{---} \text{C}_6\text{H}_4 \text{---} \text{C}(\text{CH}_3)=\text{CH} \text{---} \text{C}_6\text{H}_4 \text{---} \text{OCH}_3$	G 10 N 94 I	39

* G = glass, N = nematic, S = smectic, K = crystal, LC = liquid crystal. For example, the second polymer transforms from glass to smectic at 35 °C, from smectic to nematic at 97 °C, and from nematic to isotropic at 123 °C.

TABLE IX
COMPARISON OF ACRYLATE MONOMERS

Acrylate Monomer	Temperatures of Phase Transitions (°C)	Ref.
$(\text{CH}_3)_2\text{N}-\text{C}_6\text{H}_4-\text{CH}=\text{CH}-\text{C}_6\text{H}_4-\text{CO}(\text{CH}_2)_6\text{OCCH}=\text{CH}_2$	K 141 N 173 I	
$\text{O}_2\text{N}-\text{C}_6\text{H}_4-\text{CH}=\text{CH}-\text{C}_6\text{H}_4-\text{O}(\text{CH}_2)_6\text{OCCH}=\text{CH}_2$	K 117 I	6
$\text{O}_2\text{N}-\text{C}_6\text{H}_4-\text{CH}=\text{CH}-\text{C}_6\text{H}_4-\text{N}(\text{CH}_2)_2\text{OC}(\text{CH}_2)_5\text{OCCH}=\text{CH}_2$	K 139 N 153 I	6
$\text{NC}-\text{C}_6\text{H}_4-\text{CO}-\text{C}_6\text{H}_4-\text{O}(\text{CH}_2)_6\text{OCCH}=\text{CH}_2$	K 72 I	35
$\text{NC}-\text{C}_6\text{H}_4-\text{CH}=\text{N}-\text{C}_6\text{H}_4-\text{OC}-\text{C}_6\text{H}_4-\text{O}(\text{CH}_2)_6\text{OCCH}=\text{CH}_2$	K 94 N 233 I	35
$\text{CH}_3\text{O}-\text{C}_6\text{H}_4-\text{C}_6\text{H}_4-\text{OC}-\text{C}_6\text{H}_4-\text{O}(\text{CH}_2)_6\text{OCCH}=\text{CH}_2$	K 96 N 258 I	35
$\text{C}_6\text{H}_{16}\text{O}-\text{C}_6\text{H}_4-\text{OC}-\text{C}_6\text{H}_4-\text{O}(\text{CH}_2)_6\text{OCCH}=\text{CH}_2$	K 56 N 63 I	35
$\text{C}_6\text{H}_5-\text{CH}=\text{CH}-\text{C}_6\text{H}_4-\text{OC}-\text{C}_6\text{H}_4-\text{O}(\text{CH}_2)_6\text{OC}(\text{CH}_3)\text{CH}=\text{CH}_2$	K 99 S 165 I	37

* K = crystal, N = nematic, S = smectic, LC = liquid crystal, I = isotropic.

During the polymerization of acrylate monomers containing stilbene side chains there is a possibility to form a cross-linked polymer, if the double bond of the stilbene becomes involved in the reaction. In previous free radical polymerizations of monomers containing stilbene structural units, stilbene was very reactive towards the benzoyloxy radical at 60 °C, but was rather unreactive toward the 1-cyano-1-methylethyl radical derived from AIBN.⁴² This difference in reactivity toward the initiating radicals was ascribed to steric effects. In this experiment no evidence of polymerization of stilbene double bonds was found. Polymerization of both acrylate and stilbene double bonds would give crosslinked polymers. The polymerizations were carried out at low temperature (60-65 °C) to try to avoid cross-linking. Since all polymers were easy to dissolve in THF, dioxane and chloroform, they cannot be significantly crosslinked. The ¹H NMR spectra of the polymers in Table II and Table III also confirmed that after polymerization the ethylenic protons of the stilbene were present while the ethylenic protons of the acrylate had disappeared.

The five intermediate alcohols did not show clear evidence of liquid crystallinity. The primary hydroxyl group at the terminus of an alkyl chain may lead to a strong hydrogen bonding interaction and prevent formation of mesomorphic phases of the A-n alcohols.

While the photoisomerization is not a main research goal in the present work, and the photoisomerization of these compounds makes the syntheses more complex, it may make possible applications of these new materials, such as photo-controlled polymer liquid crystal phases, photo-controlled membrane separations, and photo-controlled polymer solution viscosities.⁴³⁻⁴⁶ These polymers might be used for photochromic probe studies of size distribution of local free volume in glassy polymer matrices.⁴⁷ It is worthwhile to continue the investigation of photoisomerization and consider the technological application of these new materials.

The UV-visible absorption of these dipolar compounds depends on the polarity of the solvent. Based on the solvent dependent frequency shift it is possible to determine the molecular second order hyperpolarizability for NLO studies.⁴⁸ *trans*-CMS has $\lambda_{\max} = 372$ nm in *n*-hexane and $\lambda_{\max} = 380$ nm in methanol. For comparison, the UV-visible absorption of 4-(N,N-dimethylamino)-4'-nitrostilbene (DANS) was also measured, and it showed $\lambda_{\max} = 418$ nm in *n*-hexane and $\lambda_{\max} = 426$ nm in methanol. DANS is a highly polarizable stilbene derivative with a large ground state dipole moment (ca. 7.5 D) which increases strongly (to ca. 25 D) in the first excited singlet state.⁴⁹ DANS is also a typical NLO organic compound which exhibits a large second order susceptibility.²¹ Since CMS and DANS have similar structures and show similar solvent dependent frequency shift, it is reasonable to expect that CMS and the new polymers have strong second order optical nonlinearity. More detailed studies on NLO properties and photochemistry of the new polymer are planned.

REFERENCES

- (1) Finkelmann, H.; Ringsdorf, H.; Wendorff, J. H. *Makromol. Chem.* **1978**, *79*, 273.
- (2) Shibaev, V. P.; Plate, N. A. Freidzon, Ya. S. *J. Polym. Sci., Polym. Chem. Ed.* **1979**, *17*, 1655.
- (3) Finkelmann, H.; Rehage, G. *Adv. Polym. Sci* **1984**, *60/61*, 99.
- (4) Shibaev, V. P; Plate, N. A. *Adv. Polym. Sci.* **1984**, *60/61*, 173.
- (5) Prasad, P. N.; Ulrich, D. R., Eds. *Nonlinear Optical and Electroactive Polymers*; Plenum Press: New York, 1988.
- (6) Griffin, A. N.; Bhatt, A. M.; Hung, R. S. L. *Proc. SPIE.* **1986**, *628*, 65.
- (7) Leslie, T. M.; Demartino, R. N.; Choe, E. W.; Khanarian, G.; Haas, D.; Nelson, G.; Stamatoff, J. B.; Stuetz, D. E.; Teng, C.; Yoon, H. *Mol. Cryst. Liq. Cryst.* **1987**, *153*, 451.
- (8) Wang, Y.; Tam, W.; Stevenson, S. H. *Chem. Phys. Lett.* **1988**, *148*, 136.
- (9) Choe, E. W. (Hoechst Celanese Co.), U. S. Patent, 4603187, 1986. *Chem. Abstr.* **1986**, *105*, 173270.

- (10) Williams, D. J., Ed. *Nonlinear Optical Properties of Organic and Polymeric Materials* (ACS Symposium Series 233), American Chemical Society, 1983.
- (11) Chemla, D. S.; Zyss, J. *Nonlinear Optical Properties of Organic Molecules and Crystals*, Academic Press: New York, 1987, vols. 1-2.
- (12) Heeger, A. J.; Orenstein, J.; Ulrich, D. R., Eds., *Nonlinear Optical Properties of Polymers*, Vol. 109, Materials Research Society: Pittsburgh, Pennsylvania, 1988.
- (13) Noel, C.; Friedrich, C.; Leonard, V.; Le Barny, P.; Ravaux, G.; Dubois, J. C. *Makromol. Chem., Macromol. Symp.* **1989**, *24*, 283.
- (14) Leslie, T. M.; Yoon, H.; Demartino, R. N.; Stamatoff, J. B. (Hoechst Celanese Co.), U. S. Patent, 4762912, 1988. *Chem. Abstr.* **1988**, *109*, 200996.
- (15) Demartino, R. N.; Yoon, H.; Stamatoff, J. B. (Hoechst Celanese Co.), European Patent, 271730, 1988. *Chem. Abstr.* **1988**, *109*, 171111.
- (16) Imura, K.; Koide, N.; Miyabayashi, M. (Mitsubishi Petrochemical Co.), Japanese Patent Application, 62-232409, 1987. *Chem. Abstr.* **1988**, *109*, 14933.
- (17) Le Barny, P. L. (Thomson-CSF S. A.), European Patent, 244288, 1987. *Chem. Abstr.* **1988**, *108*, 151153.
- (18) Singer, K. D.; Kuzyk, M. G.; Holland, W. R.; Sohn, J. E.; Lalama, S. E.; Comizzoli, R. B.; Katz, H. E.; Schilling, M. L. *Appl. Phys. Lett.* **1988**, *53*, 7.
- (19) Young, W. R.; Aviram, A.; Cox, R. J. *J. Am. Chem. Soc.* **1972**, *94*, 3976.
- (20) Young, W. R.; Haller, I.; Aviram, A. *Mol. Cryst. Liq. Cryst.* **1972**, *15*, 311.

- (21) Oudar, J. L. *J. Chem. Phys.* **1977**, *67*, 446.
- (22) Wang, Y.; Tam, W.; Stevenson, S. H.; Clement, R. A.; Calabrese, J. *Chem. Phys. Lett.* **1988**, *148*, 136.
- (23) Fouquey, C.; Lehn, J. M.; Malthete, J. *J. Chem. Soc., Chem. Commun.* **1987**, 1424.
- (24) Barbera, J.; Marcos, M.; Ros, M. B.; Serrano, J. L. *Mol. Cryst. Liq. Cryst.* **1988**, *163*, 139.
- (25) Griffin, A. C. *Mol. Cryst. Liq. Cryst.* **1976**, *34*, 111.
- (26) Emerson, W. S.; Heimsch, R. A. *J. Am. Chem. Soc.* **1950**, *72*, 5152.
- (27) Schiemenz, G. P.; Finzenhagen, M.; *Liebigs Ann. Chem.* **1981**, 1476.
- (28) Weast, R. C. Ed. *Handbook of Chemistry and Physics*, Chemical Rubber Co., **1969**, p. c-349.
- (29) Becker, K. B. *Synthesis* **1983**, 361.
- (30) Baker, R.; Sims, R. J. *Synthesis* **1981**, 117.
- (31) Weill, A.; Dechenaux, E. *Polym. Eng. Sci.* **1988**, *28*, 945.
- (32) Bornside, D. E.; Macosko, C. W.; Scriven, L. E. *J. Imaging Technology* **1987**, *13*, 122.
- (33) Stevens, H., Rehage, G.; Finkelmann, H. *Macromolecules* **1984**, *17*, 851.

- (34) Nestor, G.; White, M. S.; Gray, G. W.; Lacey, D.; Toyne, K. J. *Makromol. Chem.* **1987**, *188*, 2759.
- (35) Portugall, M.; Ringsdorf, H.; Zentel, R. *Makromol. Chem.* **1982**, *183*, 2311.
- (36) Horvath, J. *Eur. Polym. J.* **1985**, *21*, 251.
- (37) Mariam, Y. H.; Pemawansa, K. P. W.; Okoh, F.; Bota, K. B. *Mol. Cryst. Liq. Cryst.* **1986**, *141*, 77.
- (38) Bresci, V. *Makromol. Chem. Rapid Commun.* **1980**, *1*, 183.
- (39) Percec, V.; Tomazos, D. *Polym. Prepr. Am. Chem. Soc., Div. Polym. Chem.* **1988**, *29(1)*, 234.
- (40) Hampsch, H. L.; Yang, J.; Wong, G. K.; Torkelson, J. M. *Macromolecules* **1988**, *21*, 526.
- (41) Singer, K. D.; Kuzyk, M. G.; Sohn, J. E. *J. Opt. Soc. Am.* **1987**, *B4*, 968.
- (42) Bevington, J. C.; Breuer, S. W.; Huckerby, T. N. *Macromolecules* **1989**, *22*, 55.
- (43) Yamamoto, K.; Oguchi, M. (Toyobo Co.) Japanese Patent Application, 60-192712, 1985. *Chem. Abstr.* **1986**, *104*, 197694.
- (44) Anzai, J.; Hsebe, Y.; Ueno, A.; Osa, T. *J. Polym. Sci., Polym. Chem. Ed.* **1988**, *26*, 1519.
- (45) Kumano, A.; Niwa, O.; Kajiyama, T.; Takayanagi, M.; Kunitake, T.; Kano, K. *Polym. J.* **1984**, *16*, 461.

- (46) Martinez-Utrilla, R.; Catalim, F.; Sastre, R. *Makromol Chem.* **1987**, *188*, 1703.
- (47) Victor, J. G.; Torkelson, J. M. *Macromolecules* **1987**, *20*, 2951.
- (48) Buckley, A.; Choe, E.; Demartino; R. Leslie, T.; Nelson, G.; Stamatoff, J.; Stuetz, D.; Yoon, H. *Polym. Mater. Sci. Eng.* **1986**, *54*, 502.
- (49) Kawski, A.; Gryczynski, C. J.; Heckner, K. H. *Z. Naturforsch., Teil A*, **1977**, *32*, 420.

VITA

Mingyang Zhao

Candidate for the Degree of
Master of Science

Thesis: POLYACRYLATES WITH 4'-(N,N-DIMETHYLAMINO)STILBENE-4-CARBOXYLIC ESTER SIDE CHAINS

Major Field: Chemistry

Biographical:

Personal Data: Born in Beijing, China, January 10, 1950, the son of Di Zhao and Shuqin Zhao.

Education: Graduated from Qinghua University, Beijing, China, in October, 1978; received Master of Engineering Degree in Polymer Materials from Beijing Research Institute of Chemical Industry, P. R. China, October, 1984; completed requirements for the Master of Science Degree in Chemistry at Oklahoma State University in December, 1989.

Professional Experience: Technician, Beijing 3rd Chemical Factory, October, 1978 to August, 1980; Research engineer, Polymer Department, Beijing Research Institute of Chemical Industry, October, 1984 to December, 1986; Research Assistant, Department of Chemistry, Oklahoma State University, January 1987 to August 1989.